[116] Serdons, K. Evaluation of a new potential amyloid imaging agent: 6-methyl-2-(4'-[18F]fluorophenyl)-1,3-benzothiazole. *Eur. J. Nucl. Med. Mol. Imaging* **2006,** *33*, S218.

[117] Chang, Y. S.; Jeong, J. M.; Lee, Y. S.; Kim, H. W.; Ganesha, R. B.; Kim, Y. J.; Lee, D. S.; Chung, J. K.; Lee, M. C. Synthesis and evaluation of benzothiophene derivatives as ligands for imaging beta-amyloid plaques in Alzheimer's disease. *Nucl. Med. Biol.* **2006,** *33*, 811-820.

[118] Cai, L.; Chin, F. T.; Pike, V. W.; Toyama, H.; Liow, J. S.; Zoghbi, S. S.; Modell, K.; Briard, E.; Shetty, H. U.; Sinclair, K.; Donohue, S.; Tipre, D.; Kung, M. P.; Dagostin, C.; Widdowson, D. A.; Green, M.; Gao, W.; Herman, M. M.; Ichise, M.; Innis, R. B. Synthesis and evaluation of two 18F-labeled 6-iodo-2-(4'-N,N-dimethylamino)phenylimidazo[1,2-a]pyridine derivatives as prospective radioligands for beta-amyloid in Alzheimer's disease. *J. Med. Chem.* **2004,** *47*, 2208-2218.

[119] Zeng, F.; Southerland, J. A.; Voll, R. J.; Votaw, J. R.; Williams, L.; Ciliax, B. J.; Levey, A. I.; Goodman, M. M. Synthesis and evaluation of two 18F-labeled imidazo[1,2-a]pyridine analogues as potential agents for imaging beta-amyloid in Alzheimer's disease. *Bioorg. Med. Chem. Lett.* **2006,** *16*, 3015-3018.

[120] Kung, H. F.; Lee, C. W.; Zhuang, Z. P.; Kung, M. P.; Hou, C.; Plossl, K. Novel stilbenes as probes for amyloid plaques. *J. Am. Chem. Soc.* **2001,** *123*, 12740-12741.

[121] Kung, H. F. Imaging of Aβ plaques in the brain of Alzheimer's disease. *Int. Congress Series* **2004,** *1264*, 3-9.

[122] Ono, M.; Wilson, A.; Nobrega, J.; Westaway, D.; Verhoeff, P.; Zhuang, Z. P.; Kung, M. P.; Kung, H. F. C-11-labeled stilbene derivatives as A beta-aggregate-specific PET imaging agents for Alzheimer's disease. *Nucl. Med. Biol.* **2003,** *30*, 565-571.

[123] Zhang, W.; Oya, S.; Kung, M. P.; Hou, C.; Maier, D. L.; Kung, H. F. F-18 Stilbenes as PET imaging agents for detecting beta-amyloid plaques in the brain. *J. Med. Chem.* **2005,** *48*, 5980-5988.

[124] Zhang, W.; Oya, S.; Kung, M. P.; Hou, C.; Maier, D. L.; Kung, H. F. F-18 polyethyleneglycol stilbenes as PET imaging agents targeting A beta aggregates in the brain. *Nucl. Med. Biol.* **2005,** *32*, 799-809.

[125] Ono, M.; Haratake, M.; Nakayama, M.; Kaneko, Y.; Kawabata, K.; Mori, H.; Kung, M. P.; Kung, H. F. Synthesis and biological evaluation of (E)-3-styrylpyridine derivatives as amyloid imaging agents for Alzheimer's disease. *Nucl. Med. Biol.* **2005,** *32*, 329-335.

[126] Stephenson, K. A.; Chandra, R.; Zhuang, Z. P.; Hou, C.; Oya, S.; Kung, M. P.; Kung, H. F. Fluoro-pegylated (FPEG) imaging agents targeting Abeta aggregates. *Bioconjug. Chem.* **2007,** *18*, 238-246.

[127] Zhang, W.; Kung, M. P.; Oya, S.; Hou, C.; Kung, H. F. 18F-labeled styrylpyridines as PET agents for amyloid plaque imaging. *Nucl. Med. Biol.* **2007,** *34*, 89-97.

[128] Shimadzu, H.; Suemoto, T.; Suzuki, M.; Shiomitsu, T.; Okamura, N.; Kudo, Y.; Sawada, T. Novel probes for imaging amyloid-beta: F-18 and C-11 labeling of 2-(4-aminostyryl)benzoxazole derivatives. *J. Label. Compd. Radiopharm.* **2004,** *47*, 181-190.

[129] Okamura, N.; Suemoto, T.; Shiomitsu, T.; Suzuki, M.; Shimadzu, H.; Akatsu, H.; Yamamoto, T.; Arai, H.; Sasaki, H.; Yanai, K.; Staufenbiel, M.; Kudo, Y.; Sawada, T. A novel imaging probe for *in vivo* detection of neuritic and diffuse amyloid plaques in the brain. *J. Mol. Neurosci.* **2004,** *24*, 247-255.

[130] Okamura, N.; Suemoto, T.; Shimadzu, H.; Suzuki, M.; Shiomitsu, T.; Akatsu, H.; Yamamoto, T.; Staufenbiel, M.; Yanai, K.; Arai, H.; Sasaki, H.; Kudo, Y.; Sawada, T. Styrylbenzoxazole derivatives for *in vivo* imaging of amyloid plaques in the brain. *J. Neurosci.* **2004,** *24*, 2535-2541.

[131] Okamura, N.; Suemoto, T.; Furumoto, S.; Suzuki, M.; Shimadzu, H.; Akatsu, H.; Yamamoto, T.; Fujiwara, H.; Nemoto, M.; Maruyama, M.; Arai, H.; Yanai, K.; Sawada, T.; Kudo, Y. Quinoline and benzimidazole derivatives: candidate probes for *in vivo* imaging of tau pathology in Alzheimer's disease. *J. Neurosci.* **2005,** *25*, 10857-10862.

[132] Kudo, Y.; Okamura, N.; Furumoto, S.; Tashiro, M.; Furukawa, K.; Maruyama, M.; Itoh, M.; Iwata, R.; Yanai, K.; Arai, H. 2-[2-(2-Dimethylaminothiazol-5-yl)ethenyl]-6-[2-fluoroethoxy]benzoxazole (BF227): A novel PET imaging agent for *in vivo* detection of dense amyloid plaques in Alzheimer's disease patients. *J. Nucl. Med.* **2007,** *48*, 553-561.

[133] Furumoto, S.; Okamura, N.; Ishikawa, Y.; Tashiro, M.; Kato, M.; Funaki, Y.; Maruyama, M.; Akatsu, H.; Suemoto, T.; Yamamoto, T.; Arai, H.; Sawada, T.; Iwata, R.; Yanai, K.; Kudo, Y. [11C]BF227: A New 11C-Labeled 2-Ethenylbenzoxazole Derivative for Amyloid-β Plaques Imaging. *Eur. J. Nucl. Med. Mol. Imaging* **2005,** *32*, S161.

[134] Jacobson, A.; Petric, A.; Hogenkamp, D.; Sinur, A.; Barrio, J. R. 1,1-Dicyano-2-[6-(Dimethylamino)Naphthalen-2-Yl]Propene (Ddnp) - a Solvent Polarity and Viscosity Sensitive Fluorophore for Fluorescence Microscopy. *J. Am. Chem. Soc.* **1996,** *118*, 5572-5579.

[135] Liu, J.; Kepe, V.; Zabjek, A.; Petric, A.; Padgett, H. C.; Satyamurthy, N.; Barrio, J. R. High-yield, automated radiosynthesis of 2-(1-{6-[(2-[18F] fluoroethyl)(methyl)amino]-2-naphthyl}ethylidene)malononi trile ([18F] FDDNP) ready for animal or human administration. *Mol. Imaging Biol.* **2007,** *9*, 6-16.

[136] Agdeppa, E. D.; Kepe, V.; Liu, J.; Flores-Torres, S.; Satyamurthy, N.; Petric, A.; Cole, G. M.; Small, G. W.; Huang, S. C.; Barrio, J. R. Binding characteristics of radiofluorinated 6-dialkylamino-2-naphthylethylidene derivatives as positron emission tomography imaging probes for beta-amyloid plaques in Alzheimer's disease. *J. Neurosci.* **2001,** *21*, RC189.

[137] Agdeppa, E. D.; Kepe, V.; Liu, J.; Small, G. W.; Huang, S. C.; Petric, A.; Satyamurthy, N.; Barrio, J. R. 2-Dialkylamino-6-acylmalononitrile substituted naphthalenes (DDNP analogs): novel diagnostic and therapeutic tools in Alzheimer's disease. *Mol. Imaging Biol.* **2003,** *5*, 404-417.

[138] Agdeppa, E. D.; Kepe, V.; Petric, A.; Satyamurthy, N.; Liu, J.; Huang, S. C.; Small, G. W.; Cole, G. M.; Barrio, J. R. *In vitro* detection of (S)-naproxen and ibuprofen binding to plaques in the Alzheimer's brain using the positron emission tomography molecular imaging probe 2-(1-{6-(2[F-18 fluoroethyl) (methyl)amino]-2-naphthyl}ethylidene) malononitrile. *Neurosci.* **2003,** *117*, 723-730.

[139] Kung, H. F.; Kung, M. P.; Zhuang, Z. P.; Hou, C.; Lee, C. W.; Plossl, K.; Zhuang, B.; Skovronsky, D. M.; Lee, V. M.; Trojanowski, J. Q. Iodinated tracers for imaging amyloid plaques in the brain. *Mol. Imaging Biol.* **2003,** *5*, 418-426.

[140] Lee, C. W.; Kung, M. P.; Hou, C.; Kung, H. F. Dimethylamino-fluorenes: ligands for detecting beta-amyloid plaques in the brain. *Nucl. Med. Biol.* **2003,** *30*, 573-580.

[141] Chandra, R.; Kung, M. P.; Kung, H. F. Design, synthesis, and structure-activity relationship of novel thiophene derivatives for beta-amyloid plaque imaging. *Bioorg. Med. Chem. Lett.* **2006,** *16*, 1350-1352.

[142] Zhuang, Z. P.; Kung, M. P.; Kung, H. F. Synthesis of biphenyltrienes as probes for beta-amyloid plaques. *J. Med. Chem.* **2006,** *49*, 2841-2844.

[143] Shimadzu, H.; Suemoto, T.; Suzuki, M.; Shiomitsu, T.; Okamura, N.; Kudo, Y. A.; Sawada, T. A novel probe for imaging amyloid-beta: Synthesis of F-18 labelled BF-108, an Acridine Orange analog. *J. Label. Compd. Radiopharm.* **2003,** *46*, 765-772.

[144] Suemoto, T.; Okamura, N.; Shiomitsu, T.; Suzuki, M.; Shimadzu, H.; Akatsu, H.; Yamamoto, T.; Kudo, Y.; Sawada, T. *In vivo* labeling of amyloid with BF-108. *Neurosci. Res.* **2004,** *48*, 65-74.

[145] Ono, K.; Hamaguchi, T.; Naiki, H.; Yamada, M. Anti-amyloidogenic effects of antioxidants: implications for the prevention and therapeutics of Alzheimer's disease. *Biochim. Biophys. Acta* **2006,** *1762*, 575-586.

[146] Ono, K.; Hasegawa, K.; Naiki, H.; Yamada, M. Curcumin has potent anti-amyloidogenic effects for Alzheimer's beta-amyloid fibrils *in vitro*. *J. Neurosci. Res.* **2004,** *75*, 742-750.

[147] Ono, K.; Yoshiike, Y.; Takashima, A.; Hasegawa, K.; Naiki, H.; Yamada, M. Potent anti-amyloidogenic and fibril-destabilizing effects of polyphenols *in vitro*: implications for the prevention and therapeutics of Alzheimer's disease. *J. Neurochem.* **2003,** *87*, 172-181.

[148] Yang, F.; Lim, G. P.; Begum, A. N.; Ubeda, O. J.; Simmons, M. R.; Ambegaokar, S. S.; Chen, P. P.; Kayed, R.; Glabe, C. G.; Frautschy, S. A.; Cole, G. M. Curcumin inhibits formation of amyloid beta oligomers and fibrils, binds plaques, and reduces amyloid *in vivo*. *J. Biol. Chem.* **2005,** *280*, 5892-5901.

[149] Ono, M.; Yoshida, N.; Ishibashi, K.; Haratake, M.; Arano, Y.; Mori, H.; Nakayama, M. Radioiodinated flavones for *in vivo* imaging of beta-amyloid plaques in the brain. *J. Med. Chem.* **2005,** *48*, 7253-7260.

[150] Ono, M.; Maya, Y.; Haratake, M.; Nakayama, M. Synthesis and characterization of styrylchromone derivatives as beta-amyloid imaging agents. *Bioorg. Med. Chem.* **2007,** *15*, 444-450.

[151] Ryu, E. K.; Choe, Y. S.; Lee, K. H.; Choi, Y.; Kim, B. T. Curcumin and dehydrozingerone derivatives: synthesis, radiolabeling, and evaluation for beta-amyloid plaque imaging. *J. Med. Chem.* **2006**, *49*, 6111-6119.

[152] Klunk, W. E.; Engler, H.; Nordberg, A.; Wang, Y. M.; Blomqvist, G.; Holt, D. P.; Bergstrom, M.; Savitcheva, I.; Huang, G. F.; Estrada, S.; Ausen, B.; Debnath, M. L.; Barletta, J.; Price, J. C.; Sandell, J.; Lopresti, B. J.; Wall, A.; Koivisto, P.; Antoni, G.; Mathis, C. A.; Langstrom, B. Imaging brain amyloid in Alzheimer's disease with Pittsburgh Compound-B. *Ann. Neurol.* **2004**, *55*, 306-319.

[153] Arnold, S. E.; Hyman, B. T.; Flory, J.; Damasio, A. R.; Van Hoesen, G. W. The topographical and neuroanatomical distribution of neurofibrillary tangles and neuritic plaques in the cerebral cortex of patients with Alzheimer's disease. *Cereb. Cortex* **1991**, *1*, 103-116.

[154] Thal, D. R.; Rub, U.; Orantes, M.; Braak, H. Phases of A beta-deposition in the human brain and its relevance for the development of AD. *Neurology* **2002**, *58*, 1791-1800.

[155] Price, J. C.; Klunk, W. E.; Lopresti, B. J.; Lu, X.; Hoge, J. A.; Ziolko, S. K.; Holt, D. P.; Meltzer, C. C.; DeKosky, S. T.; Mathis, C. A. Kinetic modeling of amyloid binding in humans using PET imaging and Pittsburgh Compound-B. *J. Cereb. Blood Flow Metab.* **2005**, *25*, 1528-1547.

[156] Lopresti, B. J.; Klunk, W. E.; Mathis, C. A.; Hoge, J. A.; Ziolko, S. K.; Lu, X. L.; Meltzer, C. C.; Schimmel, K.; Tsopelas, N. D.; DeKosky, S. T.; Price, J. C. Simplified quantification of Pittsburgh compound B amyloid imaging PET studies: A comparative analysis. *J. Nucl. Med.* **2005**, *46*, 1959-1972.

[157] Ziolko, S. K.; Weissfeld, L. A.; Klunk, W. E.; Mathis, C. A.; Hoge, J. A.; Lopresti, B. J.; DeKosky, S. T.; Price, J. C. Evaluation of voxel-based methods for the statistical analysis of PIB PET amyloid imaging studies in Alzheimer's disease. *Neuroimage* **2006**, *33*, 94-102.

[158] Buckner, R. L.; Snyder, A. Z.; Shannon, B. J.; LaRossa, G.; Sachs, R.; Fotenos, A. F.; Sheline, Y. I.; Klunk, W. E.; Mathis, C. A.; Morris, J. C.; Mintun, M. A. Molecular, structural, and functional characterization of Alzheimer's disease: Evidence for a relationship between default activity, amyloid, and memory. *J. Neurosci.* **2005**, *25*, 7709-7717.

[159] Engler, H.; Forsberg, A.; Almkvist, O.; Blomquist, G.; Larsson, E.; Savitcheva, I.; Wall, A.; Ringheim, A.; Langstrom, B.; Nordberg, A. Two-year follow-up of amyloid deposition in patients with Alzheimer's disease. *Brain* **2006**, *129*, 2856-2866.

[160] Archer, H. A.; Edison, P.; Brooks, D. J.; Barnes, J.; Frost, C.; Yeatman, T.; Fox, N. C.; Rossor, M. N. Amyloid load and cerebral atrophy in Alzheimer's disease: an 11C-PIB positron emission tomography study. *Ann. Neurol.* **2006**, *60*, 145-147.

[161] Edison, P.; Archer, H. A.; Hinz, R.; Hammers, A.; Pavese, N.; Tai, Y. F.; Hotton, G.; Cutler, D.; Fox, N.; Kennedy, A.; Rossor, M.; Brooks, D. J. Amyloid, hypometabolism, and cognition in Alzheimer disease: an [11C]PIB and [18F]FDG PET study. *Neurology* **2007**, *68*, 501-508.

[162] Fagan, A. M.; Mintun, M. A.; Mach, R. H.; Lee, S. Y.; Dence, C. S.; Shah, A. R.; LaRossa, G. N.; Spinner, M. L.; Klunk, W. E.; Mathis, C. A.; DeKosky, S. T.; Morris, J. C.; Holtzman, D. M. Inverse relation between *in vivo* amyloid imaging load and cerebrospinal fluid A beta(42) in humans. *Ann. Neurol.* **2006**, *59*, 512-519.

[163] Mintun, M. A.; Larossa, G. N.; Sheline, Y. I.; Dence, C. S.; Lee, S. Y.; Mach, R. H.; Klunk, W. E.; Mathis, C. A.; DeKosky, S. T.; Morris, J. C. [11C]PIB in a nondemented population: potential antecedent marker of Alzheimer disease. *Neurology* **2006**, *67*, 446-452.

[164] Verhoeff, N.; Wilson, A. A.; Takeshita, S.; Trop, L.; Hussey, D.; Singh, K.; Kung, H. F.; Kung, M. P.; Houle, S. In-vivo imaging of Alzheimer disease beta-amyloid with. *Am. J. Geriatr. Psychiatry* **2004**, *12*, 584-595.

[165] Shoghi-Jadid, K.; Small, G. W.; Agdeppa, E. D.; Kepe, V.; Ercoli, L. M.; Siddarth, P.; Read, S.; Satyamurthy, N.; Petric, A.; Huang, S. C.; Barrio, J. R. Localization of neurofibrillary tangles and beta-amyloid plaques in the brains of living patients with Alzheimer disease. *Am. J. Geriatr. Psychiatry* **2002**, *10*, 24-35.

[166] Barrio, J. R.; Kepe, V.; Satyamurthy, N.; Huang, S.-C.; Small, G. W. Brain pathology and neuronal losses in the living brain of Alzheimer's patients. *Int. Congress Series* **2006**, *1290*, 150-155.

[167] Small, G. W.; Kepe, V.; Ercoli, L. M.; Siddarth, P.; Bookheimer, S. Y.; Miller, K. J.; Lavretsky, H.; Burggren, A. C.; Cole, G. M.; Vinters, H. V.; Thompson, P. M.; Huang, S. C.; Satyamurthy, N.; Phelps, M. E.; Barrio, J. R. PET of brain amyloid and tau in mild cognitive impairment. *N. Engl. J. Med.* **2006**, *355*, 2652-2663.

Received: February 22, 2007 Accepted: March 20, 2007

Geriatr Gerontol Int 2007; 7: 393–400

ORIGINAL ARTICLE: BIOLOGY

Binding and safety profile of novel benzoxazole derivative for *in vivo* imaging of amyloid deposits in Alzheimer's disease

Nobuyuki Okamura,[1] Shozo Furumoto,[2] Yoshihito Funaki,[3] Takahiro Suemoto,[4] Motohisa Kato,[1] Yoichi Ishikawa,[3] Satoshi Ito,[1] Hiroyasu Akatsu,[5] Takayuki Yamamoto,[5] Tohru Sawada,[4] Hiroyuki Arai,[6] Yukitsuka Kudo[2] and Kazuhiko Yanai[1]

[1]Department of Pharmacology, Tohoku University Graduate School of Medicine, [2]Tohoku University Biomedical Engineering Research Organization (TUBERO), [3]Division of Radiopharmaceutical Chemistry, Cyclotron and Radioisotope Center, Tohoku University, [6]Center for Asian Traditional Medicine, Department of Geriatrics and Gerontology, Tohoku University School of Medicine, Sendai, [4]BF Research Institute, Osaka, and [5]Fukushimura Hospital, Toyohashi, Japan

Background: *In vivo* detection of amyloid deposits in the brain is potentially useful for early diagnosis of Alzheimer's disease (AD) and tracking the efficacy of anti-amyloid therapy.

Methods: To develop an amyloid-binding agent for positron emission tomography, we screened over 2600 compounds.

Results: We found benzoxazole derivatives as candidate compounds for *in vivo* amyloid imaging probes. One of these agents, 2-(2-[2-dimethylaminothiazol-5-yl]ethenyl)-6-(2-[fluoro]ethoxy)benzoxazole (BF-227), displays high binding affinity to Aβ fibrils. BF-227 binding increased linearly with increasing Aβ fibril formation. In temporal and hippocampal AD brain sections, BF-227 selectively bound to amyloid plaques. In contrast, no staining was evident in the cerebellum. Compared with the previously reported compound BF-168, ^{18}F-labeled BF-227 displayed selective *in vivo* labeling of amyloid fibrils and rapid washout from white matter areas in an Aβ-injected rat model. An acute and subacute toxicity study of BF-227 indicated sufficient safety for clinical use as a positron emission tomography probe.

Conclusions: These findings suggest that BF-227 is feasible as an *in vivo* imaging probe of amyloid deposits in AD patients.

Keywords: Alzheimer's disease, amyloid, positron emission tomography, senile plaques.

Introduction

Progressive deposition of senile plaques (SP) and neurofibrillary tangles (NFT) is a critical event in the pathogenesis of Alzheimer's disease (AD). These lesions precede the presentation of clinical symptoms of dementia.[1] For early or presymptomatic diagnosis of AD, non-invasive detection of these lesions using positron emission tomography (PET) is a potentially

Accepted for publication 22 August 2007.

Correspondence: Dr Nobuyuki Okamura MD PhD, Department of Pharmacology, Tohoku University Graduate School of Medicine, 2-1 Seiryo-machi, Aoba-ku, Sendai 980-8575, Japan. Email: oka@mail.tains.tohoku.ac.jp

doi: 10.1111/j.1447-0594.2007.00430.x

useful technique.[2] To achieve successful *in vivo* imaging using PET, sensitive and selective contrast agents to these lesions are needed. Congo red and thioflavin T have represented attractive lead compounds as developing amyloid-imaging agents, because these compounds selectively bind to β-pleated sheet structures and are commonly used for histochemical staining of SP. However, the permeability of these compounds through the blood–brain barrier (BBB) is extremely limited.[3] The chemical structure must thus be optimized to provide appropriate lipophilicity without changing the binding properties to amyloid. Thioflavin T derivatives without any positive charge show high permeability of the BBB. One of these compounds, 6OH-BTA-1 (PIB), has been applied in a human PET study and enabled successful detection of early AD patients.[4] Another compound, 2-(1-[6-[<2-fluoroethyl><methyl>amino]-2-naphthyl]ethylidene) malononitrile (FDDNP), is extremely lipophilic and can easily penetrate the BBB, and specifically binds to both SP and NFT in AD brain sections.[5] After i.v. injection of FDDNP, greater accumulation was observed in SP- and NFT-rich areas of the human brain.[6] Although validation is still required as to whether retention of these agents in the neocortex truly reflects levels of amyloid deposition, such findings suggest the potential usefulness of this technique for early diagnosis of AD.

We have previously demonstrated a novel series of compounds including 6-(2-fluoroethoxy)-2-(2-[4-methylaminophenyl]ethenyl)benzoxazole (BF-168) and (2-[4-methylaminophenyl]ethenyl)-5-fluorobenzoxazole (BF-145) as promising candidates for *in vivo* imaging probes of SP.[7–9] These benzoxazole derivatives demonstrate high binding affinity for Aβ aggregates and high BBB permeability, suggesting potential utility as *in vivo* amyloid-binding agents. However, for the application of these compounds to clinical PET studies, the pharmacokinetic properties and pharmacological safety of these molecules requires improvement. This study describes the characterization of an optimized benzoxazole derivative, 2-(2-[2-dimethylaminothiazol-5-yl]ethenyl)-6-(2-[fluoro]ethoxy) benzoxazole (BF-227), as a candidate *in vivo* amyloid-imaging agent in humans.

Methods

Preparation of the compounds

BF-168, BF-227 (Fig. 1) and the precursor compounds for ^{18}F-labeled agents were custom-synthesized by Tanabe R & D Service (Osaka, Japan). Synthesis of (^{18}F)BF-168 was performed by reacting 2-(4-methylaminophenyl)-6-(2-tosyloxyethoxy) benzoxazole (Tanabe R & D Service) with (^{18}F)KF and Kryptofix 222 (Merck, Darmstadt, Germany) in acetonitrile at 80°C for 20 min, as described previously.[8] Radiosynthesis of (^{18}F)BF-227 was performed using the same method. After subsequent high-performance liquid chromatography (HPLC) purification, ^{18}F-labeled compounds were obtained (Fig. 1). Details of the radiosynthetic methods will be described elsewhere.

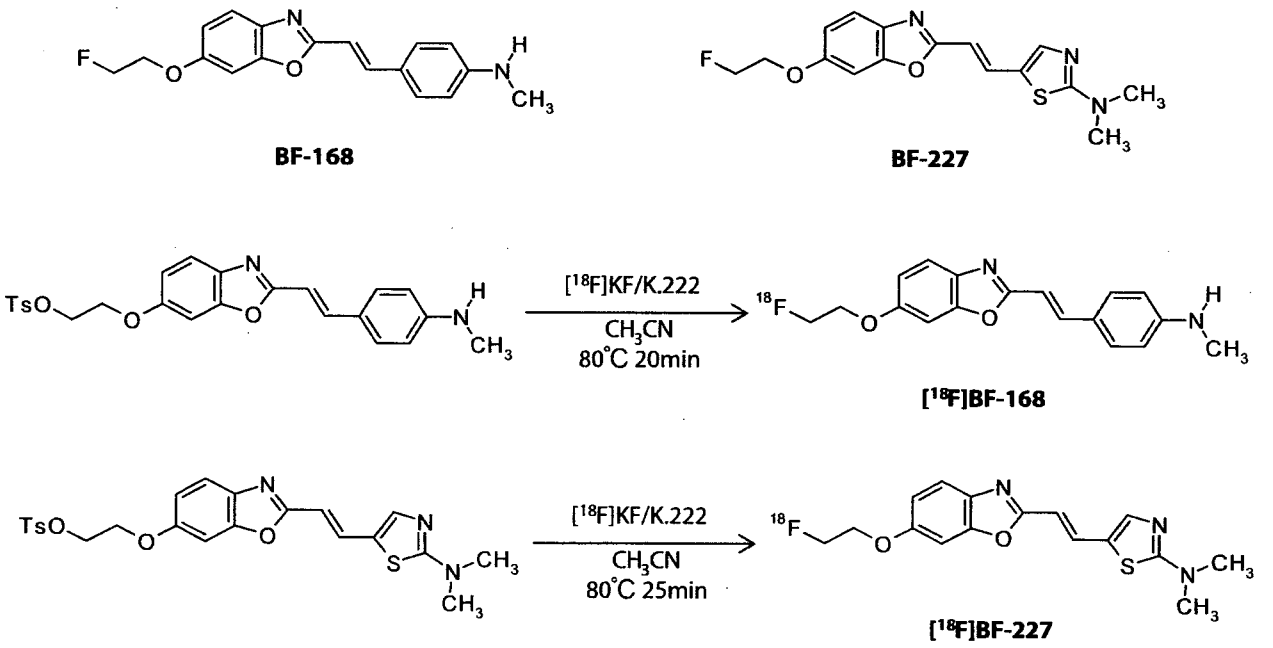

Figure 1 Chemical structures and radiosynthesis of BF-168 and BF-227.

In vitro *binding assays*

Binding affinities of the compounds for synthetic Aβ aggregates were examined as described previously.[7] Briefly, solid-form Aβ1–40 (Peptide Institute, Osaka, Japan) was dissolved in 10 mmol/L potassium phosphate buffer (pH 7.4) and incubated at 37°C for 72 h. The binding assay was performed by mixing aggregated Aβ1–40 with the appropriate concentration of ^{18}F-labeled BF-227, unlabeled BF-227 and dimethyl sulfoxide. After incubation for 10 min at room temperature, the binding mixture was filtered using a cell harvester (Model M-24; Brandel, Gaithersburg, MD, USA) and filters containing bound ^{18}F ligand were counted using a γ-counter. The dissociation constant (K_d) of BF-227 was determined by Scatchard analysis.

Fluorometric analysis of BF-227 binding with Aβ fibrils was performed using the following method. A total of 20 μmol/L of Aβ1–40 or Aβ1–42 (Peptide Institute) in 50 mmol/L of potassium phosphate buffer (pH 7.4) was incubated at 37°C on a Vibrax VXR shaker (IKA, Cincinnati, OH, USA) at 0.56 *g*. Before fluorometric analysis, Aβ solutions were sonicated for 3 min at 45 kHz using a VS-100III ultrasonic cleaner (Iuchi, Osaka, Japan). In fluorometry, Aβ1–40 and Aβ1–42 solutions at 0, 4, 8 and 24 h after the start of incubation were mixed with the same volume of BF-227 solution (5 μmol/L final concentration). After determination of the optimal excitation wavelength for the mixture of BF-227 and Aβ, fluorescence spectra were measured using a Gemini XS microplate spectrofluorometer (Molecular Devices, Sunnyvale, CA, USA). In addition, fluorescence spectra for the mixture of 5 μM BF-227 and different concentrations of Aβ1–40 or Aβ1–42 (0.15, 0.5 1.5, 2.5, 5 and 10 μmol/L final concentrations) at 96 h after incubation (fibrillar Aβ) were measured using the microplate spectrofluorometer. The same measurements were also performed using Aβ1–40 and Aβ1–42 with no incubation (non-fibrillar Aβ). All measurements were performed in triplicate.

Neuropathological staining

Postmortem brain tissues from an autopsy-confirmed AD case (69-year-old man) were obtained from Fukushimura Hospital (Toyohashi, Japan). Experiments were performed under the regulations of the Ethics Committee of BF Research Institute. Serial sections (6-μm thick) from paraffin-embedded blocks of temporal cortex and cerebellum were prepared in xylene and ethanol. Before staining, quenching of autofluorescence was performed as described previously. Quenched tissue sections were immersed in 100 μmol/L of BF-227 solution for 10 min or 0.01% 1-bromo-2,5-bis(3-carboxy-4-hydroxystyryl)benzene (BSB) solution containing 50% ethanol for 30 min. Sections stained with BF-227 were then dipped briefly into water and rinsed in phosphate-buffered saline (PBS) for 60 min before coverslipping with Fluor Save Reagent (Calbiochem, La Jolla, CA, USA), and examined using an Eclipse E800 microscope (Nikon, Tokyo, Japan) equipped with a V-2A filter set (excitation 380–420 nm, dichroic mirror 430 nm, longpass filter 450 nm). Sections stained with BSB were dipped briefly in tap water and then in 50% ethanol, then washed in PBS for 60 min before coverslipping, followed by fluorescent microscopy using a BV-2A filter set (excitation 400–440 nm, dichroic mirror 455 nm, longpass filter 470 nm). In addition, adjacent sections were immunostained using monoclonal antibody (mAb) against Aβ (6F/3D; Dako A/S, Glostrup, Denmark). After pretreatment with 90% formic acid for 5 min, sections were immersed in blocking solution for 30 min and then incubated for 60 min at 37°C with 6F/3D at a dilution of 1:50. Following incubation, sections were processed by the avidin–biotin method using a Pathostain ABC-POD(M) Kit (Wako, Osaka, Japan) and diaminobenzidine tetrahydrochloride. Fluorescence intensity of three different brain slices stained with BF-227 was analyzed by defining regions of interest (ROI) and measuring the intensity of fluorescence within gray and white matter using Lumina Vision software (Mitani, Fukui, Japan). Ratios of gray matter ROI to white matter ROI were calculated as an indicator of stainability and statistical comparisons were performed using ANOVA and Scheffe post-hoc tests.

Labeling of amyloid deposits in Aβ-injected rat model

Aβ1–40 (Peptide Institute) was dissolved at 500 μmol/L in 50 mmol/L potassium phosphate buffer and incubated at 37°C for 4 days. An Aβ-injected rat model was created as described previously.[10] Briefly, Wistar rats (male, 200–250 g, SLC, Shizuoka, Japan) were injected with Aβ peptides unilaterally and potassium phosphate buffer contralaterally into each amygdala using a stereotaxic instrument (Model 5000, David Kopf, Tujunga, CA, USA). Injection coordinates measured from the bregma and skull surface (anteroposterior, −3.0 mm; mediolateral, ±5.0 mm; dorsoventral, −8.8 mm) were determined based on a stereotaxic atlas.[11] A volume of 1.0 μL was administered over 2 min using a microsyringe and glass cannula (tip diameter, 170–250 μm). At 3 days after injection of Aβ and vehicle, (^{18}F)BF-168 (72.8 MBq) or (^{18}F)BF-227 (58.9 MBq) were administered into the femoral vein of anesthetized rats. Rats were killed by decapitation at 180 min postinjection and the brains were removed and frozen. An OTF cryostat (Bright Instruments, Huntingdon, UK) was used to cut 30-μm thick frozen sections, which were then dried and exposed to a BAS-III imaging plate for 18 h. Autoradiographic images were obtained using a BAS2000 scanner system

(Fuji Film, Tokyo, Japan). After autoradiographic examination, the same sections were stained with thioflavin-S to confirm the presence of amyloid plaques.

Toxicity study in mice

A non-GLP (good laboratory practice) toxicity study was performed using female and male ICR mice (weight, 22–32 g). The Ethics Committee of BF Research Institute approved the protocol for these experiments. Animals were kept in a temperature-controlled environment (21.2–23.5°C) with a 12-h light–dark cycle and ad libitum access to food and water. In the acute toxicity study, animals were divided into one control group and three treated groups, with 10 animals (five males, five females) in each group. The control group received injection of vehicle alone, while each treated group received i.v. injection of BF-227 solution in doses of 0.1, 1 or 10 mg/kg. Animals were observed for 8 days after administration to identify any changes in general behavior or bodyweight. In the subacute toxicity study, animals were divided into one control group and two treated groups (2.5 and 25 μg/kg), with 10 animals (five females, five males) in each group. The control group received injection of vehicle alone and each treated group received i.v. injection of BF-227 solution for 14 days (once daily). Animals were weighed at 3, 7, 9 and 14 days after administration. At the end of the experiment, animals were sacrificed and examined at autopsy. Selected organs (brain, heart, liver, lung and kidney) were removed, weighed and examined microscopically by a pathologist.

Results

Binding characteristics of BF-227 for Aβ fibrils

In vitro binding assay indicated that BF-227 shows high binding affinity for Aβ fibrils. K_d for Aβ1–40 fibrils was 1.0 ± 1.4 nmol/L, comparable to previously reported levels for amyloid imaging agents[12] (Fig. 2). Binding ability of BF-227 to Aβ was also examined by fluorometric analysis, as BF-227 is highly fluorescent. In the mixture of BF-227 and Aβ peptides, fluorescence intensity of BF-227 increased as Aβ1–40 (Fig. 3a) and Aβ1–42 (data not shown) incubation time advanced. BF-227 fluorescence also increased in a linear manner with increasing concentrations of fibrillar Aβ1–42 (Fig. 3b) or Aβ1–40 (data not shown), but did not increase in mixture with non-fibrillar Aβ. These results suggest that degree of BF-227 binding reflects the amount of Aβ fibril formation.

Neuropathological staining in AD brain sections

Neuropathological examination using BF-227 indicated that amyloid plaques were clearly stained with BF-227

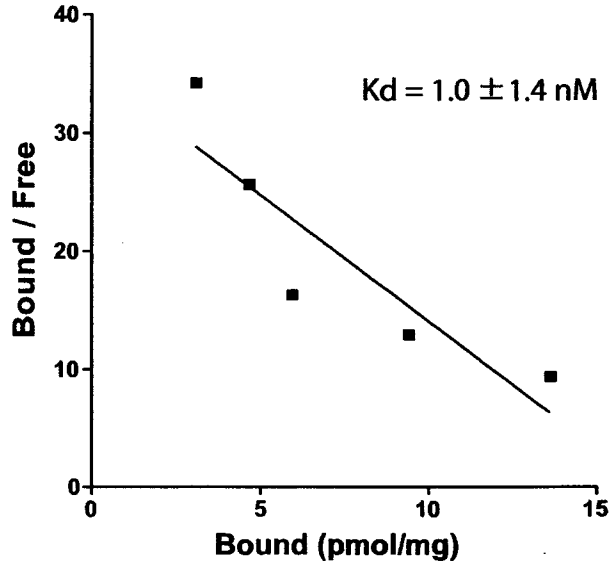

Figure 2 Scatchard plots of (^{18}F)BF-227 binding to synthetic Aβ fibrils.

in AD brain sections (Fig. 4a). In particular, cored plaques stained brightly with this compound. This staining pattern correlated well with Aβ immunostaining in adjacent sections (Fig. 4b). BF-227 staining was further compared to staining using BSB, a Congo red derivative. In contrast to clear staining of SP and NFT with BSB (Fig. 4c), BF-227 primarily stained SP, with faint staining of NFT. Preferential binding of BF-227 to SP rather than NFT represents a similar characteristic to the previously reported compound BF-145. BF-227 staining was subsequently performed in three different regions (temporal lobe, hippocampus and cerebellum) of an AD brain. In temporal (Fig. 5a) and hippocampal (Fig. 5b) sections, cored plaques stained brightly with BF-227. In contrast, no staining was evident in the cerebellum (Fig. 5c). Fluorometric measurement of these brain sections indicated that overall level of stainability in the cerebellum differed significantly from that in the temporal cortex and hippocampus (Fig. 5d), suggesting the binding specificity of this compound to AD pathology.

Intravenous administration of ^{18}F-labeled agents in Aβ-injected rat model

In vivo binding ability of (^{18}F)BF-168 and (^{18}F)BF-227 to Aβ fibrils was further evaluated by the autoradiographic experiment in the Aβ-injected rat model. In an image of the brain section at 180 min postinjection of ^{18}F-labeled agents (Fig. 6), Aβ aggregates were clearly labeled with both agents, suggesting the usefulness of these agents as *in vivo* amyloid-imaging probes. However, non-specific

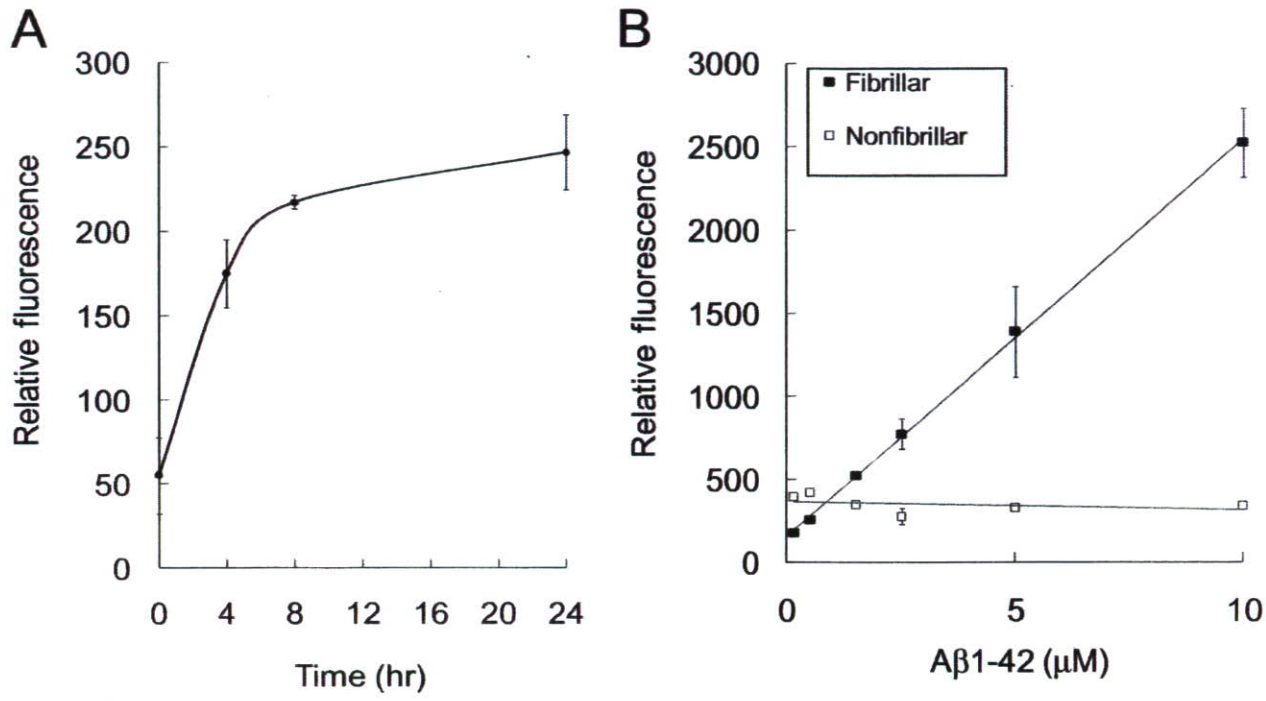

Figure 3 *In vitro* binding of BF-227 with Aβ peptides. Fluorescence intensity of BF-227 increased with Aβ incubation time (A). BF-227 fluorescence also increased linearly with concentrations of fibrillar Aβ, but did not increase in mixture with non-fibrillar Aβ (B).

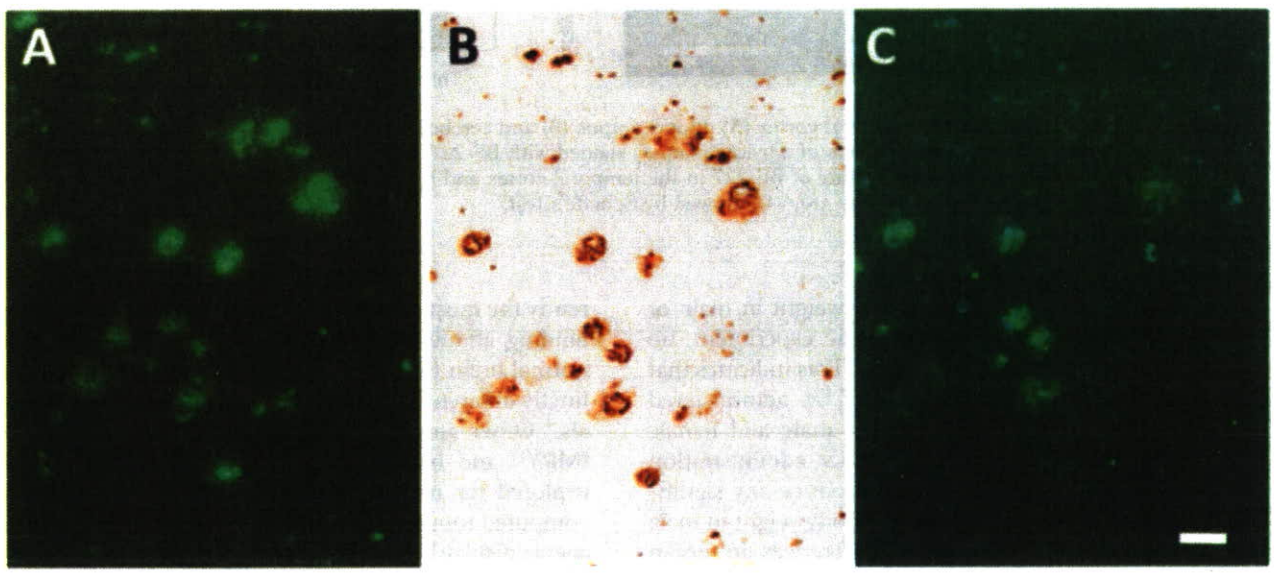

Figure 4 Neuropathological staining of Alzheimer's disease (AD) temporal brain sections by BF-227. Senile plaques are clearly stained with BF-227 (A). This staining correlates well with Aβ immunostaining in adjacent sections (B). BSB stains both senile plaques and neurofibrillary tangles (C). Bar, 200 μm.

retention of (^{18}F)BF-227 in the white matter was much less than that of (^{18}F)BF-168. This resulted in better hot spot-to-background contrast for (^{18}F)BF-227 (Fig. 6b) compared to (^{18}F)BF-168 (Fig. 6a).

Toxicity study of BF-227

In the acute toxicity study, i.v. administration of BF-227 in doses 0.1–10 mg/kg did not produce any significant

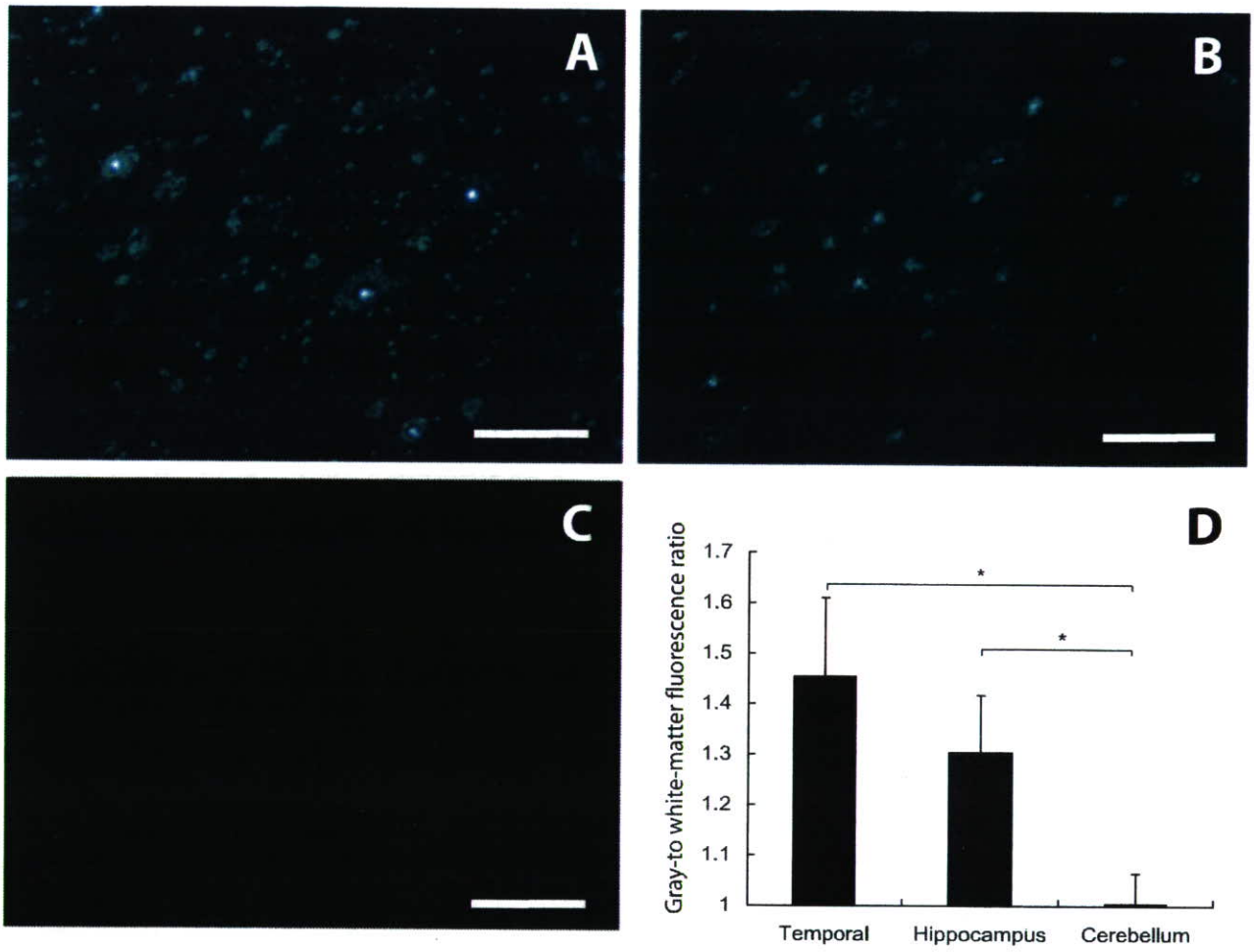

Figure 5 BF-227 staining in the temporal cortex (A), hippocampus (B) and cerebellum (C) of AD brain. In temporal and hippocampal brain sections, large numbers of amyloid plaques stained with BF-227. In contrast, no apparent staining was observed in the cerebellum. The stainability of BF-227 in the temporal cortex and hippocampus differed significantly from that in the cerebellum (D). $*P < 0.05$, one-way ANOVA followed by Scheffe's test.

changes in general behavior or bodyweight in male or female mice. During the 8 days of the experiment, no deaths occurred in any of the groups. This indicates that the dose for 50% lethality (LD_{50}) of i.v. administered BF-227 is higher than 10 mg/kg for male and female mice. In the subacute toxicity study, i.v. administration of BF-227 in tested doses did not produce any significant changes in general behavior or bodyweight in male or female mice. No significant differences in organ weight were observed between control and BF-227-administered groups. After the 14-day post-treatment period, mice did not show any microscopic alterations on pathological examination.

Discussion

Several research groups have worked to develop amyloid-imaging agents for use with PET. PIB is currently the most successful of these agents, showing high binding affinity for Aβ fibrils and fast clearance from normal brain tissue.[13] In the clinical trial, PIB-PET distinctly differentiated AD patients from normal individuals.[4] Other amyloid-imaging agents, such as SB-13,[14] IMPY[15] and benzofuran derivatives,[16] have also been explored for use as PET and single-photon emission computed tomography (SPECT) imaging probes. These agents display high binding affinity to Aβ fibrils. The key chemical structure common to these imaging agents is an aminophenyl group, which is considered essential for binding to the β-pleated sheet structure of Aβ fibrils. The present study, however, demonstrated that BF-227, a derivative of BF-168 with an aminothiazol group in place of the aminophenyl group, also binds strongly to amyloid-β fibrils. Furthermore, an autoradiographic study comparing BF-227 to BF-168 suggested that the aminothiazol group might contribute in a large way to

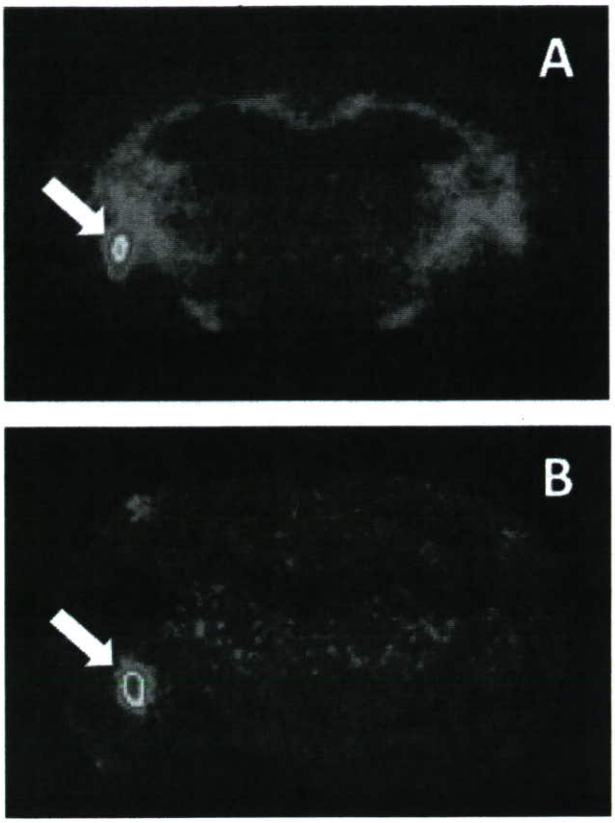

Figure 6 *In vivo* labeling of Aβ fibrils in brain sections from the Aβ-injected rat model with (^{18}F)BF-168 (A) and (^{18}F)BF-227 (B). Arrows indicate sites of Aβ injection.

decreased non-specific retention in normal brain tissue, particularly in white matter. This possibility should be examined in further studies, as this finding would be helpful in the design or modification of further series of amyloid-imaging agents.

Findings from the *in vitro* binding experiment indicated that the amount of BF-227 binding is proportional to the concentration of Aβ fibrils. Neuropathological findings also indicated that BF-227 preferentially binds to lesions containing dense Aβ fibrils. Densities of neuritic plaques are higher in the temporal, parietal and occipital lobes, moderate in the limbic lobe and lowest in the cerebellum.[17] Our results for BF-227 stainability in different brain regions were consistent with this neuropathological pattern of Aβ deposition in AD patients. Brains from patients with AD are characterized by an anatomically widespread process of amyloid deposition. Presence of neuritic or cored plaques is considered the best indication of the presence of the disease process underlying AD.[18] Quantitative measurement of Aβ fibril formation using BF-227 will thus allow discrimination of the disease process from normal aging processes. SP in the cerebellum are predominantly of the non-fibrillar type. The lack of obvious staining by BF-227 in the cerebellum thus suggests the binding preference of this compound to fibrillar Aβ.

The present study demonstrated high binding affinity of BF-227 to fibrillar Aβ and preferential binding to SP in AD brain sections. i.v. administration of this compound into an Aβ-injected rat model demonstrated selective binding to amyloid fibrils in the brain and faster clearance from white matter than BF-168. The toxicity study indicated that BF-227 is safe for clinical use as a PET probe, with a very wide margin between the lethal dose of BF-227 (>10 mg/kg) and clinical dose in human PET studies (<100 ng/kg). Considering all these findings together, BF-227 appears applicable for use as an *in vivo* amyloid-imaging agent. We are currently engaging in a clinical PET trial using ^{11}C-labeled BF-227 in AD patients.[19] This trial will elucidate the clinical utility of BF-227 in humans.

Acknowledgments

This study was partially supported by the Novartis Foundation for Gerontological Research, the Special Coordination Funds for Promoting Science and Technology, the Program for the Promotion of Fundamental Studies in Health Science by the National Institute of Biomedical Innovation, the Industrial Technology Research Grant Program from the New Energy and Industrial Technology Development Organization (NEDO) of Japan, Health and Labor Sciences Research Grants for Translational Research from the Japanese Ministry of Health, Labor and Welfare, a JST grant on research and education in molecular imaging, and an Astrazeneca Research Grant.

References

1 Price JL, Morris JC. Tangles and plaques in nondemented aging and "preclinical" Alzheimer's disease. *Ann Neurol* 1999; **45**: 358–368.
2 Nordberg A. PET imaging of amyloid in Alzheimer's disease. *Lancet Neurol* 2004; **3**: 519–527.
3 Klunk WE, Wang Y, Huang GF, Debnath ML, Holt DP, Mathis CA. Uncharged thioflavin-T derivatives bind to amyloid-beta protein with high affinity and readily enter the brain. *Life Sci* 2001; **69**: 1471–1484.
4 Klunk WE, Engler H, Nordberg A *et al.* Imaging brain amyloid in Alzheimer's disease with Pittsburgh Compound-B. *Ann Neurol* 2004; **55**: 306–319.
5 Agdeppa ED, Kepe V, Liu J *et al.* Binding characteristics of radiofluorinated 6-dialkylamino-2-naphthylethylidene derivatives as positron emission tomography imaging probes for beta-amyloid plaques in Alzheimer's disease. *J Neurosci* 2001; **21**: RC189.
6 Small GW, Kepe V, Ercoli LM *et al.* PET of brain amyloid and tau in mild cognitive impairment. *N Eng J Med* 2006; **355**: 2652–2663.
7 Okamura N, Suemoto T, Shimadzu H *et al.* Styrylbenzoxazole derivatives for in vivo imaging of amyloid plaques in the brain. *J Neurosci* 2004; **24**: 2535–2541.

8 Shimadzu H, Suemoto T, Suzuki M *et al.* Novel probes for imaging amyloid-β: F-18 and C-11 labeling of 2-(4-aminostyryl) benzoxazole derivatives. *J Label Compd Radiopharm* 2004; **47**: 181–190.
9 Okamura N, Suemoto T, Shiomitsu T *et al.* A novel imaging probe for in vivo detection of neuritic and diffuse amyloid plaques in the brain. *J Mol Neurosci* 2004; **24**: 247–255.
10 Suemoto T, Okamura N, Shiomitsu T *et al.* In vivo labeling of amyloid with BF-108. *Neurosci Res* 2004; **48**: 65–74.
11 Paxinos G, Watson C. *The Rat Brain in Stereotaxic Coordinates*. San Diego, CA: Academic Press, 1998.
12 Mathis CA, Klunk WE. Imaging β-amyloid plaques and neurofibrillary tangles in the aging human brain. *Curr Pharm Design* 2004; **10**: 1469–1492.
13 Mathis CA, Wang Y, Holt DP, Huang GF, Debnath ML, Klunk WE. Synthesis and evaluation of ^{11}C-labeled 6-substituted 2-arylbenzothiazoles as amyloid imaging agents. *J Med Chem* 2003; **46**: 2740–2754.
14 Verhoeff NP, Wilson AA, Takeshita S *et al.* In-vivo imaging of Alzheimer disease beta-amyloid with [^{11}C]SB-13 PET. *Am J Geriatr Psychiatry* 2004; **12**: 584–595.
15 Kung MP, Hou C, Zhuang ZP *et al.* Characterization of IMPY as a potential imaging agent for β-amyloid plaques in double transgenic PSAPP mice. *Eur J Nucl Med Mol Imaging* 2004; **31**: 1136–1145.
16 Ono M, Kawashima H, Nonaka A *et al.* Novel benzofuran derivatives for PET imaging of β-amyloid plaques in Alzheimer's disease brain. *J Med Chem* 2006; **49**: 2725–2730.
17 Arnold SE, Hyman BT, Flory J, Damasio AR, Van Hoesen GW. The topographical and neuroanatomical distribution of neurofibrillary tangles and neuritic plaques in the cerebral cortex of patients with Alzheimer's disease. *Cereb Cortex* 1991; **1**: 103–116.
18 Price JL. Diagnostic criteria for Alzheimer's disease. *Neurobiol Aging* 1997; **18**: S67–S70.
19 Kudo Y, Okamura N, Furumoto S *et al.* 2-[2-(2-dimethylaminothiazol-5-yl) ethenyl] -6-[2-(fluoro) ethoxy-]benzoxazole: a novel PET imaging agent for in vivo detection of dense amyloid plaques in Alzheimer's disease patients. *J Nucl Med* 2007; **48**: 553–561.

Expert Opinion

informa
healthcare

General

Experimental treatments for human transmissible spongiform encephalopathies: is there a role for pentosan polysulfate?

NG Rainov†, Y Tsuboi, P Krolak-Salmon, A Vighetto & K Doh-ura
†*Klinikum Augsburg, Department of Neurosurgery, Stenglinstr. 2, D-86156 Augsburg, Germany, and Martin-Luther-University Halle-Wittenberg, Department of Neurosurgery, D-06122 Halle, Germany*

Human transmissible spongiform encephalopathies (TSEs), also known as prion diseases, are caused by the accumulation of an abnormal isoform of the prion protein in the CNS. Creutzfeldt-Jakob disease in its sporadic form is the most frequent type of human TSE. At present, there is no proven specific or effective treatment available for any form of TSE. Pentosan polysulfate (PPS) has been shown to prolong the incubation period when administered to the cerebral ventricles in a rodent TSE model. Cerebroventricular administration of PPS has been carried out in 26 patients with TSEs and has been shown to be well tolerated in doses ≤ 220 µg/kg/day. Proof of efficacy has been difficult because the specific and objective criteria for measurement of response have not been established yet. Preliminary clinical experience confirms extended survival in patients with variant Creutzfeldt-Jakob disease receiving intraventricular PPS; however, it is still not clear if this is due to PPS itself. Further prospective investigations of long-term intraventricular PPS administration are essential for the assessment of its effects.

Keywords: Gerstmann-Straussler-Scheinker syndrome, pentosan polysulfate, prion disease, quinacrine, sporadic Creutzfeldt-Jakob disease, transmissible spongiform encephalopathy, variant Creutzfeldt-Jakob disease

Expert Opin. Biol. Ther. (2007) 7(5):xxx-xxx

1. Introduction

Transmissible spongiform encephalopathies (TSEs), also known as prion diseases, have a common and unique biological background. All forms of TSEs share an abnormal metabolism of the prion protein, PrP^{c}, which results in the production of protease-resistant isoforms, PrP^{sc}, accumulating mostly in the CNS and causing neuronal dysfunction and eventually death [1,2]. The underlying pathological process involves a post-translational conformational change of PrP^{c} into PrP^{sc} [3,4]. PrP is usually present in an α-helix-rich conformation (PrP^{c}), but in pathological conditions only a small fraction of PrP is folded as α-helix-rich PrP^{c}, and the vast majority is present in a β-helix-rich conformation (PrP^{sc}) [5]. The claim that PrP^{sc} is an infective agent involves the demonstration that the PrP^{sc} form can itself modify the structure of PrP^{c} to PrP^{sc} *in vitro*; however, this modification is rather inefficient [6]. Recent results suggest that single-stranded RNA molecules are necessary for PrP^{c} to PrP^{sc} conversion, and that RNA from invertebrates fails to support this conversion *in vitro* [7]. PrP^{sc} molecules build up in a cell-associated manner and some of them are seen extracellularly as amyloid deposits in histopathological sections. Microglia is activated by contact with amyloid plaques and insoluble extracellular PrP^{sc}, which results in local production and release of cytokines, reactive oxygen species and

glutamate [8,9]. These compounds may give rise to neuronal damage and spongiform degeneration in the brain.

Physiological neuronal activity is expected to be severely impaired well in advance of histopathological changes. The progressive, slow build up of PrP^{sc} may mean that only tissues where cells are not involved in a continuous turnover are likely to exhibit functional and morphological damage. Although some cells of the immune system are also infected by PrP^{sc}, their cellular turnover may be considered to prevent the body showing any dysfunction of the immune system, whereas neurons infected with accumulated PrP^{sc} are damaged, but not replaced, and hence long-term neurological deficits become clinically manifested [10].

Activation of astrocytes occurs in a consistent fashion very early in the course of prion infection of the CNS. It leads to significant physiological effects, such as impairment of the blood–brain barrier (BBB) [11]. In addition, astrocytes are one of the few cell types capable of supporting prion replication [12]. Microglial cells are another cell type increasingly implicated in brain damage due to prion infection. Microglial activation and accumulation in affected brain areas precede neuronal cell death and match the temporal and spatial pattern of PrP^{sc} deposition [13]. Histologically, common late-stage lesions in the CNS are neuronal loss, spongiosis and astrogliosis, accompanied by an accumulation of microglia and, occasionally, the presence of amyloid plaques and various small deposits of prion protein [14,15].

TSEs demonstrate variable clinical manifestations, all of which are presumably based on the above common pathogenetic mechanisms and can affect both humans and animals. In humans, TSEs include such conditions as Creutzfeldt-Jakob disease (CJD), Gerstmann-Straussler-Scheinker syndrome (GSS), fatal familial insomnia (FFI) and the now extinct kuru. Sporadic CJD was originally described in 1921 and occurs mostly in individuals between 40 and 80 years of age, with an incidence of approximately one case/one million of the population/year. Patients suffering from CJD show a wide spectrum of clinical symptoms within a few distinctive forms of the disease [16]. Although most of the CJD cases at present are sporadic, CJD may also occur as a familial form in ≤ 10% of sporadic cases [17]. It follows an autosomal dominant pattern of inheritance, with the patients having a mutation in codons such as codon 178 or 200 of the *prion protein* (*PRNP*) gene. Iatrogenic transmission of CJD has been proven in > 400 cases in relation to corneal transplants, dura mater grafts and hormones purified from human pituitary glands [18-20]. FFI and GSS are also inherited by autosomal dominance and are related to missense mutations of the *PRNP* gene. Both are relatively rare, with < 10 reported families with FFI and 50 with GSS [21,22]. Unlike other TSEs, GSS may have a longer clinical course [23]. It is characterised by specific neuropathological lesions and multicentric amyloid plaques.

The most recently recognised form of TSEs in humans, variant CJD (vCJD), was first described in 1996 as being linked to bovine spongiform encephalopathy (BSE) [24]. The characteristics that distinguish vCJD from sporadic cases (sCJD) is that the age of patients is much lower (vCJD age range: 19 – 39 years, versus sCJD age range: 55 – 70 years) and the duration of illness is longer (vCJD: 7.5 – 22 months, versus sCJD: 2.5 – 6.5 months). vCJD displays a distinct pathology, which is characterised by abundant florid plaques surrounded by vacuolation. In addition, all investigated cases of vCJD showed homozygosity of methionine at codon 129 [25-27]. Most cases of vCJD have been observed in the UK.

The clinical features of TSEs are extremely heterogeneous and may include rapidly progressive dementia (mostly in sporadic CJD), psychiatric symptoms (mostly in vCJD, but less in sporadic CJD), cerebellar syndrome (in kuru, GSS and vCJD), movement disorders (myoclonus, dystonia and chorea, mostly in vCJD), encephalopathy (in sporadic CJD), pyramidal signs, cortical blindness (mostly in sporadic CJD) and sensory symptoms (hyperpathia mostly in vCJD) [16,23,27-29].

2. Experimental treatments for human transmissible spongiform encephalopathies

TSEs are still uniformly fatal, some within weeks to months from diagnosis, while vCJD patients may survive for > 1 year, and GSS patients for ≤ 6 years. Animal studies indicate that, with all TSEs, substantial neuropathological changes are already present before the onset of symptoms and are spatially related to PrP^{sc} deposits. Therefore, an effective intervention should ideally start during the preclinical stage of disease and be aimed at preventing PrP^{sc} neuroinvasion or propagation in the CNS. Unfortunately, no tests are available to detect asymptomatic TSEs at present, except for carriers of pathogenic mutations of the *PRNP* gene.

No specific treatments for TSEs are known, although some prophylactic and neuroprotective agents have been proposed on the basis of cell culture experiments and animal studies [30-34]. However, most compounds that have shown some effectiveness in cell culture or animal models of TSEs only work when administered at the time of infection or shortly thereafter. The heterogeneity and complexity of TSEs suggest that a combination of several compounds with different modes of action may be necessary for their treatment. As an example, combination therapies have been successful in other incurable and fatal diseases (AIDS or cancer). Therefore, disease progression could be halted or delayed by the synergistic effects of different agents against distinct targets in the misfolding pathway. Kocisko *et al.* (2006) [35] reported that combination treatment beginning 14 or 28 days after scrapie inoculation with two different drugs in mice significantly increased survival times. The authors implied that the compounds act synergistically *in vivo*.

2.1 Antibiotics, dyes and *N*-methyl-D-aspartate receptor ligands

The polyene macrolide antibiotic amphotericin B [36,37] and its less toxic derivative MS-8209 [38] have been shown to delay

scrapie agent propagation and PrP^{sc} accumulation in mice or hamsters. The amyloid-binding dye, Congo red, is able to inhibit PrP^{sc} accumulation and replication [39], most probably by overstabilising the abnormal conformational isoform [40]. The anthracycline 4-iodo-4-deoxy-doxorubicin has been found to delay hamster scrapie progression via binding to amyloid fibrils [41]. Suramin, a highly sulfated urea-based compound, and dapsone, a sulfone, were also tested against mouse scrapie and were found to increase the incubation period when given continuously [42,43]. Porphyrins and phthalocyanins as sulfated forms also were shown to inhibit the production of PrP^{sc} in neuroblastoma cell cultures [44,45].

The neurotoxic effect displayed by PrP^{sc} and its fragments was found to be prevented *in vitro* by antagonists of the widely distributed ligand-gated *N*-methyl-D-aspartate (NMDA) ion channel, such as memantine [8,46]. Moreover, flupirtine, a triaminopyridine compound clinically used as a non-opioid analgesic drug, which acts like an NMDA receptor antagonist, but does not bind to the receptor, was found to display a strong cytoprotective effect on neurons treated with PrP^{sc} or with a toxic fragment [46,47]. Flupirtine was also found to enhance the intracellular levels of the antiapoptotic protein Bcl-2 and the antioxidative agent glutathione.

A double-blind placebo-controlled study has been carried out in 28 CJD patients [48]. Patients treated with flupirtine showed significantly less cognitive changes (dementia) than placebo patients, which led the authors to conclude that flupirtine may have beneficial effects on the cognitive function of patients with CJD [48]. The study did not investigate other aspects of neurological deterioration or overall survival in progressive CJD.

2.2 Quinacrine and chlorpromazine

The antimalarial drug quinacrine (mepacrine), a cyclic tetrapyrrole, and the antipsychotic drug chlorpromazine were shown to prevent the conversion of PrP^{c} to PrP^{sc} in cell culture. Doh-ura *et al.* (2000) [49] reported that lysosomotropic agents (e.g., quinacrine or chloroquine) inhibited protease-resistant prion protein accumulation in scrapie-infected murine neuroblastoma cells. The inhibition occurred without apparent effects on normal PrP^{c} biosynthesis or turnover, and without direct interactions with prion protein molecules. Similar effects of quinacrine were reported later by Korth *et al.* (2001) [50] . These authors cultured similar types of scrapie-infected murine neuroblastoma cells to show that 6 days of treatment with quinacrine or chlorpromazine was able to reduce the conversion of PrP^{c} to PrP^{sc}.

Quinacrine has been used in humans for > 60 years to treat malaria and can be administered orally at high doses on a daily basis. At present, the suggested oral dose for CJD patients is higher than the antimalarial dose and may produce significant side effects in a considerable proportion of the treated patients. Chlorpromazine, although less potent than quinacrine in cell culture, crosses the BBB to a greater extent.

Turnbull *et al.* (2003) [51] showed that quinacrine also may act as an effective antioxidant, readily scavenging hydroxyl radicals generated during incubation of toxic PrP 106-126 peptide fragment with murine neurons. On the other hand, Collins *et al.* (2002) [52] evaluated oral quinacrine in an experimental murine model of TSE, but were not able to demonstrate any significant effect of the drug on overall survival of treated animals compared with controls. Barret *et al.* (2003) [53] also examined the efficacy of quinacrine and chlorpromazine in different *in vitro* models and in an experimental murine model of BSE. Despite the inhibition of PrP^{sc} accumulation in scrapie-infected murine neuroblastoma cells, quinacrine was unable to produce a detectable effect in the animal model. Martinez-Lage *et al.* (2005) [54] described a case of iatrogenic CJD (dural graft) where therapy with quinacrine and chlorpromazine failed to improve the clinical condition. Haik *et al.* [55] (2004) reported the results of an open compassionate use study of quinacrine in 32 patients with sporadic CJD. In some genotypic subgroups, a slight but nonsignificant increase in survival was observed, which was probably due to biased inclusion of long-term surviving patients. There was no evidence of a beneficial effect of quinacrine treatment.

Japanese researchers are carrying out an ongoing clinical study of oral quinacrine in patients with sporadic and iatrogenic CJD. Results in the first four patients have been published recently [56]. Quinacrine 300 mg/day has been administered for 3 months. Improved arousal level of patients with akinetic mutism, and restored eye contact or voluntary movements in response to stimuli were described. However, clinical improvement was transient, lasting 1 – 2 months. Quinacrine at the above dose caused liver dysfunction and skin pigmentation in all cases [56]. Further results in a larger patient population are expected in the near future.

A prospective clinical study of quinacrine in TSEs (the PRION-1 study [101]) has just finished enrolling patients in the UK. Patients aged ≥ 12 years with all types of TSEs were eligible. The study protocol featured a partially randomised design, with patients opting for quinacrine treatment split into two arms according to their preference for immediate versus deferred (by 24 weeks) treatment. Treated patients received a loading dose of quinacrine (1 g on the first day), followed by 300 mg/day as a long-term dose. The primary efficacy end points were mortality and the proportion of responders overall and at 24 weeks. Response was defined as independently rated lack of deterioration, global impression of change (based on the Clinician's Interview-Based Impression of Change-plus) and the patient's score on the Brief Psychiatric Rating Scale. Secondary efficacy end points were neurological and neuropsychological changes, including changes in markers of disease activity, magnetic resonance imaging (MRI) and electroencephalography [101].

Routine follow-up was identical for all patients participating in the PRION-1 trial, with the exception of patients with inherited TSE, who have longer disease duration

and were followed up less frequently. Follow-up assessments took place monthly for the first 6 months then every 3 months until end of study. Assessments included medical history, physical examination, liver function and blood clotting, neurological examination recorded on video and a series of neurological assessments. The study accrual target was 160 patients. However, the study enrolled a total of 81 patients until closure in June 2006. Final results of the study remain to be reported and are not in the public domain at present.

2.3 Polysulfonated glycosides (glycans)

Several polysulfonated polysaccharides, including pentosan polysulfate (PPS) and dextran sulfate, have been shown to prolong the incubation period in scrapie-infected rodents if given before infection [57-59] and to inhibit PrP^{sc} accumulation in neuroblastoma cells [60]. The effects of these polyanions may be due to an inhibition of the formation of PrP fibrils [61] or due to a reduction of the amount of PrP^{c} on the cell surface by stimulating endocytosis of PrP^{c} [44]. Sulfonated polyglycosides are not known to penetrate the CNS; hence, the first attempts to demonstrate their effects were made in peripheral organs [62].

Caughey and Raymond (1993) [60] tested various polysulfonated glycosides and found PPS, carrageenan and dextran sulfate 500 (DS500) to be highly active at inhibiting PrP^{sc} production. PPS was most active, showing half of its maximal activity at 1 ng/ml. Shyng *et al.* (1995) [44] reported that PPS and related compounds cause a decrease of PrP^{c} on the surface of cultured chicken and mouse neuroblastoma cells. PPS caused a redistribution of PrP^{c} from the surface to the interior of the cell (intracellular late endosomes). The differences in the binding strength of PrP^{c} to PPS and to other polysulfonated glycosides were found to parallel their *in vivo* and *in vitro* anti-PrP^{sc} formation potency. Ehlers and Diringer (1984) [63] inoculated mice intraperitoneally or intracerebrally with scrapie agent and treated them systemically with DS500. None of the intracerebrally inoculation experiments were affected by the treatment. With intraperitoneal inoculations, however, it was seen that DS500 did decrease (by approximately one order of magnitude) the infectivity found in the spleen at various times after single injection of the drug, and significantly prolonged incubation times. Treated mice also showed a significant increase in the mean incubation period compared with controls. It was noted that DS500 remained in the body of an inoculated mouse for ≤ 7 months. A maximum effect was seen when the drug was given at the same time as the infection, and no effect was seen when it was given 35 days after infection [63].

This work was followed by the study of Farquhar and Dickinson (1986) [62], who carried out a series of murine experiments to intraperitoneally inoculate with scrapie pathogens. This was associated, at various times before and after the pathogen inoculation, with various quantities of DS500 as a single intraperitoneal injection. It was found that DS500 reliably increased the incubation period of the disease and this did not seem to depend on the scrapie pathogen strains or the inbred strains of mouse used. The effect seemed to be present when DS500 was given ≤ 4 weeks before and ≤ 3 weeks after the pathogen inoculation. The incubation period was extended by 5 – 19% at this dose, but if increased doses of DS500 were used, the incubation period could be prolonged by $\leq 62\%$ [62]. Kimberlin and Walker (1986) [64] gave various inocula of scrapie to mice either intravenously or intraperitoneally, and various drugs were tested before or after the scrapie infection. DS500 proved to be effective in reducing the titre of the scrapie infectivity. Little effect was seen with heparin, dextran or diethylaminoethyl dextran. Diringer and Ehlers (1991) [57] inoculated mice intraperitoneally with scrapie pathogen and administered PPS intraperitoneally on different days (days 84 – 50) before the infection. PPS increased the incubation period of mice by up to 75%. Hamsters were also intraperitoneally inoculated with various quantities of DS500 or PPS and with a scrapie pathogen, separated by 2 – 24 hrs [65]. As the dose of DS500 increased the incubation period also increased, but the maximum increase achieved with non-toxic doses of the drug was 21%. It was noted that a single intraperitoneally administration of PPS increased the incubation period of intracerebrally inoculated scrapie by ~ 18% [65]. Farquhar *et al.* (1999) [66] injected intraperitoneally PPS immediately after scrapie infection of mice. Depending on mouse strain, a single PPS 250 mg dose increased the scrapie incubation period by up to 66%. A single 1-mg intraperitoneal dose of PPS protected mice completely from simultaneous scrapie infection. On the other hand, oral PPS was ineffective at delaying disease.

Doh-ura *et al.* (2004) [67] recently intracerebrally infected transgenic mice expressing hamster prion protein with hamster-adapted scrapie pathogen, and different agents were infused cerebroventricularly starting on either day 10 or day 35 after infection. The infusion was continued for 4 weeks. Infused drugs included amphotericin B, PPS and lysosomotropic chemicals, such as E-64d cysteine protease inhibitor, chloroquine and quinacrine. Lysosomotropic agents demonstrated no significant effect in prolonging the incubation time when administered on either day 10 or day 35 after infection. Amphotericin B resulted in ~ 30% prolongation of the incubation time when administered at the early stage, but no significant prolongation at the late stage. PPS showed the most beneficial effects, and mice that received PPS at the early stage survived 141% longer, and at the late stage they survived 71% longer. Maximal effects of PPS at a later stage (day 42 of infection) were obtained at 230 µg/kg/day. Analysis of the detailed relationship between the initiation time of the infusion of PPS and outcome revealed that the effects of PPS were quite dependent on the timing of infusion initiation, with earlier initiation of treatment

rendering a better prognosis [67]. Analysis with either immunohistochemistry or immunoblotting demonstrated that PPS potently inhibited PrP^{sc} deposition in the brain hemisphere implanted with the PPS infusion cannula. Immunohistochemical analysis demonstrated that mice treated with PPS from the early stage showed no PrP^{sc} deposits on day 52 within the hemisphere implanted with the infusion cannula, and a very small amount of deposits even at the terminal stage, day 142. On the other hand, control animals demonstrated PrP^{sc} deposits in the parahippocampal white matter on day 35, and later on, at day 52, also in the thalamus and hypothalamus. No notable adverse effects were observed in experimental mice treated with PPS ≤ 230 μg/kg/day intraventricular for 2 months. In a separate set of experiments in normal dogs, higher doses, such as 345 and 460 μg/kg/day, did show adverse effects, such as partial or generalised epileptic seizures, which began within 24 h after the start of PPS infusion [67].

Both heparin and PPS are rapidly taken up into the reticuloendothelial system (RES) cells by a saturable pathway. Low doses are cleared quickly into the RES, whereas higher doses saturate the RES and are excreted in the urine [68]. PPS is metabolised by cellular nonspecific desulfation in many organs and tissues, including vascular endothelium [69]. Renal excretion of desulfated PPS from plasma takes place over 6 days following a single dose, which also involves partial polyxylose chain breakdown. PPS can be administered orally, but only a low proportion (0.5 – 4%) of the drug is detected in the blood circulation [70,71]. When PPS is given orally, anti-inflammatory effects are seen in the bladder after long-term administration [72]. It is considered that this is due to accumulation of the drug caused by slow breakdown and excretion in cells of the RES. When used for anticoagulation and given subcutaneously or intravenously, PPS may cause an early, benign, reversible thrombocytopenia and a rise in lipoprotein lipase activity [70]. Similarly to heparin, a rare, immune, severe form of thrombocytopenia has also been reported [73]. No significant neurological symptoms or signs have been reported in humans or animals treated with PPS orally or parenterally.

There has been no CNS penetration demonstrated with peripherally administered PPS, which is not surprising due to the hydrophilic nature of the drug. On the other hand, direct intracerebral administration of PPS may afford high compartmental concentrations of the drug in the CNS, but no pharmacokinetics are available for this specific mode of administration. Direct administration of PPS to the CNS would be expected to allow PPS into concentrate in cells with ubiquitous heparan-binding sites and to exert effects on those cells infected with prion. In analogy to other therapeutic molecules (e.g., recombinant proteins delivered directly into the primate and human brain [74,75]), it is considered probable that cerebroventricular infusion of PPS may have the highest ratio of local versus systemic drug concentration.

3. Rationale for local administration of drugs to the cerebrospinal fluid

The clinical and late preclinical phase of TSE with PrP^{sc} formation in the brain requires drugs that can cross into brain parenchyma and be present in the brain in a biologically active concentration [23,33]. However, in the early stages of TSE, with an intact BBB, there is a severe limitation of penetration of drugs from blood into brain interstitium, and from there into glial and neuronal cells. Even at late stages of the disease, tight junctions of the brain capillaries may remain at least partially intact, therefore selectively limiting the entry of most molecules.

Compounds that are highly lipid soluble, such as alcohol, barbiturates and some anticonvulsants, may easily pass through the endothelial cells forming the inner layer of the BBB. Lipid solubility is measured by the oil/water (octanol/water) partition coefficient, and molecules with a high coefficient usually efficiently permeate the BBB (for review see [76]). Examples of highly lipid-soluble compounds with a high partition coefficient are phenytoin and methadone, which cross the BBB in large quantities under normal conditions. However, not all lipid-soluble molecules easily traverse the BBB. Compounds highly bound to plasma proteins have restricted access to the brain. For these substances, the degree of dissociation of the protein complex in transit through the capillary bed determines the degree of penetration across the BBB. Furthermore, there are special transport systems that are responsible for enhanced passage of certain compounds with low lipid solubility across the BBB, such as the physiologically important molecules D-glucose and phenylalanine [77]. The BBB can be subjected to pharmacological or osmotic modifications aimed at temporarily increasing its permeability to certain therapeutic molecules. However, these approaches are invasive and have the potential for serious side effects [78,79].

The cerebrospinal fluid (CSF)–brain barrier seems to be more permeable because of its anatomical structure, which lacks tight junctions between the neuroependymal cells lining the cerebral ventricles. Substances administered to the CSF have been shown to penetrate into brain tissue by diffusion. The physical process of diffusion is gradient-driven, and penetration of the CSF–brain barrier will be enhanced by the higher concentration of a molecule in one compartment [80,81]. This fact points at an important advantage of the local application of drugs to the CSF: high local concentration in the CNS compartments, as opposed to negligible systemic concentration due to low reabsorption in the bloodstream.

Continuous CSF circulation is a physiological process that lends itself to the dissemination of substances throughout the CNS. CSF is continuously produced and completely replaced in the brain approximately every 8 h. In normal adults, the rate of CSF removal by reabsorption is equal to the rate of CSF production by filtration of blood through the

intraventricular choroid plexus. CSF circulates from the sites of production, the lateral ventricles and third ventricle, into the cerebral aqueduct and into the fourth ventricle. From there, CSF escapes the internal ventricular system of the brain by the foramina of Luschka and Magendie, and into the subarachnoid space around the brain and the spinal cord. Arachnoid granulations and dural sinuses are the route for CSF reabsorption to the blood circulation [82].

In a model of cerebroventricular infusion in rats, radioactive sucrose was infused into one lateral ventricle. Minutes after infusion, sucrose moved into the third ventricle, the aqueduct, the fourth ventricle, and the subarachnoid space of the quadrigeminal, ambient and interpeduncular cisterns. Approximately 15% of the injected sucrose entered these large cisterns. In contrast to most other CSF–brain interfaces, a small amount of sucrose moved from CSF the into the medulla next to the lateral recesses and tissues adjacent to the large CSF cisterns. A thick, multilayered glia limitans visible on electron micrographs seemed to form a CSF–brain barrier at these interfaces [83].

Evidence also exists for the bulk flow of brain interstitial fluid via preferential pathways through the brain, which is closely related to CSF. This bulk flow of interstitial fluid has implications for drug delivery, drug distribution and drug clearance [84].

4. Preliminary results with continuous long-term intraventricular administration of pentosan polysulfate in human transmissible spongiform encephalopathies

At present, the objective of cerebroventricular PPS administration in TSE patients is aimed at evaluating the short- and long-term safety and tolerability of escalating doses of PPS administered by continuous long-term infusion. A secondary objective is to assess efficacy of PPS in delaying or halting disease progression and improving existing neurological deficits. Patients with probable sporadic, iatrogenic or variant CJD, or with hereditary syndromes such as GSS or FFI, are eligible to receive PPS infusion. Informed consent is obtained from patients or legally appointed representatives.

The primary end point of early PPS administration studies was a maximum tolerated dose of PPS as assessed by the occurrence of serious toxicity resulting from PPS administration. Dose-limiting toxicity was defined as any one of the following occurring in two or more patients:

- any grade 4 toxicity attributed to PPS
- grade 3 toxicity for either neurological symptoms or symptoms in other organ systems lasting > 5 days and attributed to PPS

Patients considered for PPS administration had to have a probable diagnosis of one of the above TSEs in accordance to WHO criteria. Normal haematological, renal and liver function was also a requirement. Due to the surgical procedure for implantation of the ventricular catheter, subcutaneous pump and infusion system, ongoing treatment with anticoagulants such as warfarin, heparin, clopidogrel or aspirin was not allowed. In addition, the presence of any active infection or any viral syndrome within 2 weeks prior to treatment was an exclusion criterion.

Patients undergoing surgery had ventricular catheters placed in the anterior horn of the right lateral ventricle (or in a few cases in both frontal horns), unless clinical reasons dictated another point of access to the ventricular system. In the first case of intraventricular PPS administration, the catheter was connected initially to an external pump for trial administration of PPS, and later attached to a subcutaneously programmable pump (Synchromed EL 18 ml, Medtronic, Inc., Minneapolis, MN, USA) permanently implanted in the abdominal subcutaneous tissue. Later cases had simultaneous implantation of the catheter system and the infusion pump in the same surgical session. A total of 3 – 14 days after the surgical procedure, in which time the pump was not active and scar tissue formation was expected to occur, PPS infusion commenced at a low dose level. The decision to proceed to the next higher dose level was based on the absence of clinical side effects and on normal findings on non-enhanced computed tomography (CT) scans (e.g., exclusion of hydrocephalus or intracranial blood).

There are no previously published data on a safe or potentially effective dose of intraventricularly infused PPS in human patients with TSE. Based on preclinical animal work, a dose-escalation schedule was set up starting at 1 μg/kg/day and escalating on a daily basis until a target dose of 11 μg/kg/day was reached. This represented a 10-fold dose reduction based on body surface area and weight differences from the lowest effective PPS dose used in scrapie-infected mice in a preclinical study of intraventricular PPS [67]. The maximum daily dose of intraventricular PPS administered to the first six patients on a long-term basis was 11 μg/kg/day. Further cases have received maximum doses of up to 220 μg/kg/day in a few escalation steps, but long-term follow-up experience with doses > 110 μg/kg is still limited (Table 1).

The source of PPS for human use is Pentosanpolysulfat SP54 in sterile 1-ml vials (Bene Arzneimittel GmbH, Munich, Germany). Each vial contains 100 mg of sodium-PPS (100 mg/ml) with 1% sodium-4-oxopentanate as a stabiliser. For filling of the pump reservoir, PPS SP54 100 mg/ml is diluted with 0.9% sodium chloride to a final concentration of 1 – 10 mg/ml. The pump is then programmed to deliver the total daily dose in a continuous simple infusion mode (constant volume and infusion rate over time).

There are no standardised or widely accepted criteria for assessment of the treatment efficacy in TSE. Thus, surrogate criteria for efficacy were thus adopted and included overall survival, speed of disease progression before PPS infusion compared with disease progression after start of PPS, neuroradiological imaging, and changes in the general and neurological condition of the patients.

Table 1. Summary of clinical data of all present patients with PPS administration .

Patient number	Sex	Age at Dx* (years)	Diagnosis and clinical course	Survival (months after Tx*)	Maximum PPS dose (μg/kg/d)
1	M	17	vCJD. Stable disease, swallowing and myoclonus improved, brain stem function improved. PPS started at very advanced stage of disease.	48	11
2	M	19	sCJD. Initial neurological improvement, weight gain, reduction of myoclonus. Later slow progression Seizures a few months after start of PPS. PPS stopped 20 months after start of administration.	32	11
3	F	19	vCJD. Stable disease, wheelchair bound. At present, stable weight, speech deficit, swallowing fluids, PEG.	35	11
4	M	18	vCJD. PPS started at a late stage of disease. Initially some deterioration, then stable disease.	35	32
5	F	44	GSS. Oral PPS for 5 years prior to i.v. PPS. Stable disease but surgical complications (brain haemorrhage) causing neurological deficits. Died of infection unrelated to PPS	27*	11
6	F	39	GSS. Oral PPS for 5 years prior to i.v. PPS. Stable disease. Initially only very mild neurological symptoms present.	25	11
7	F	37	Iatrogenic CJD (GH administration) Cerebellar syndrome, initially stable condition. Later slow deterioration.	28	110
8	F	27	Iatrogenic CJD (GH administration) Rapid progression before start of PPS, slower progression afterwards. Died of pneumonia.	19*	110
9	F	42	vCJD. Continuous neurological deterioration on PPS. Generalized seizures 2 months after start of PPS. Died of systemic complications.	4*	110
10	M	44	GSS. Continuous neurological deterioration. Increase in mental symptoms and disorientation while on PPS. Died of septicaemia.	10*	110
11	M	34	Iatrogenic CJD (GH administration) Progressive disease. Died of general complications (aspiration pneumonia).	3*	110
12	F	47	GSS. Mild neurological deficits at start of PPS. Some improvement of speech initially. Later increased gait ataxia, decline of short-term memory. Cause of death unknown.	11*	110
13	F	67	sCJD. Treatment started at an advanced stage of disease. Progression of disease while on PPS. Died of sepsis.	17*	120
14	F	73	sCJD. Treatment started early in the course of disease. Slow progression of disease while on PPS. PPS stopped after a few months due to subdural collections and seizures. Died of pneumonia.	20*	120
15	M	49	sCJD PPS started at a very late clinical stage. Stable disease, but subdural collections on CT scans.	20	220
16	F	68	sCJD (MM2). Treatment started at a late clinical stage. Stable condition on PPS.	19	120
17	F	64	fCJD (V180I). Treatment started early in the course of the disease. Subdural collections at 7 months of treatment, PPS reduced to 60 μg/kg/d. Stable condition on PPS.	19	120

* Patient deceased.

CJD: Creutzfeldt-Jakob disease; Dx: Diagnosis; F: Female; fCJD: Familial CJD; GH: Growth hormone; GSS: Gerstmann-Straussler-Scheinker syndrome; i.v.: Intravenous; M: Male; PEG: Polyethylene glycol; PPS: Pentosan polysulfate; sCJD: Sporadic CJD; Tx: Therapy; vCJD: Variant CJD.

Table 1. Summary of clinical data of all present patients with PPS administration (continued).

Patient number	Sex	Age at Dx* (years)	Diagnosis and clinical course	Survival (months after Tx*)	Maximum PPS dose (μg/kg/d)
18	F	64	sCJD. Progression of disease while on PPS. PPS stopped due to bilateral subdural collections.	14	120
19	M	37	fCJD (200). Treatment started lately in the course of the disease. Died of systemic complications.	3*	110
20	M	37	iCJD (GH administration). Died of general complications (aspiration pneumonia). Bilateral subdural collections discovered at 10 months of treatment, PPS reduced to 60 μg/kg/d, stopped 1 month prior to death.	12*	110
21	F	60	sCJD. Died of disease progression.	2*	110
22	M	56	iCJD (dura mater implantation 1987). Slow progression on PPS. Died of pneumonia.	4*	120
23	M	66	iCJD (dura mater implantation 1981). Neurological deterioration while on PPS.	7	120
24	F	69	GSS (P102L) Cognitively not impaired, but ataxic gait and mild dysarthria. Stable condition on PPS.	5	120
25	M	30	iCJD (GH administration). Treatment started late in the disease. Died from disease progression.	1.5*	110
26	F	45	sCJD. Slow deterioration since start of PPS.	3	110

* Patient deceased.

CJD: Creutzfeldt-Jakob disease; Dx: Diagnosis; F: Female; fCJD: Familial CJD; GH: Growth hormone; GSS: Gerstmann-Straussler-Scheinker syndrome; i.v.: Intravenous; M: Male; PEG: Polyethylene glycol; PPS: Pentosan polysulfate; sCJD: Sporadic CJD; Tx: Therapy; vCJD: Variant CJD.

4.1 Clinical cases

The first patient to receive PPS infusion was a young man suffering from vCJD [85]. He presented initially at the age of 16 years with subjective signs of behavioral disturbance, followed a few months later by progressive ataxia, pyramidal signs and myoclonus, which led to the clinical diagnosis of possible vCJD. The clinical picture combined with abnormal MRI findings (pulvinar sign) and positive tonsil biopsy allowed the diagnosis of probable vCJD 8 months after the occurrence of initial clinical symptoms. At the time of first administration of PPS (14 months after diagnosis), the patient had symptoms of advanced vCJD, such as ataxia, dementia, dysphagia, dysphasia and myoclonus, and was confined to bed and unable to care for himself. He was fed via percutaneous gastrostomy. A catheter was implanted in the anterior horn of the right lateral ventricle and connected to a programmable pump (Synchromed EL, Medtronic) implanted subcutaneously in the abdomen. The initial PPS dose of 1 μg/kg/day was escalated without drug-related complications to the target dose of 11 μg/kg/day. Intraventricular administration of PPS at the above dose did not have any measurable systemic anticoagulant activity in serum, as confirmed by unchanged international normalised ratio before and during PPS infusion. Follow-up CT scans demonstrated no intracerebral haemorrhage (Figure 1) and there were no seizures. Subdural fluid collection, first over the right hemisphere and subsequently over the left hemisphere, necessitated surgical (burr hole) evacuation of fluid. Repeated surgical revisions of the fluid collections were carried out.

At present, this first patient is still alive in a stable and unchanged neurological condition. PPS has been administered intraventricularly for 44 months. Although there were no major improvements in the neurological and general conditions, there were a few notable changes. The swallow reflex was restored and the myoclonus was reduced a few weeks after start of PPS administration. The patient has gained weight compared with pre-PPS baseline while on the same nutritional regime. Regular follow-up CT scans have shown progressive brain atrophy during the first 2 years of PPS administration, which reached a plateau phase after that time (Figure 1). However, advancing brain atrophy could not be correlated to any worsening of the clinical condition (Figures 1 and 2). Observations in this and other cases suggest that the timeframe for developing cortical/subcortical brain atrophy (as seen on MRI or CT scans) lags behind the clinical manifestation of symptoms. Initially, progressing neurological

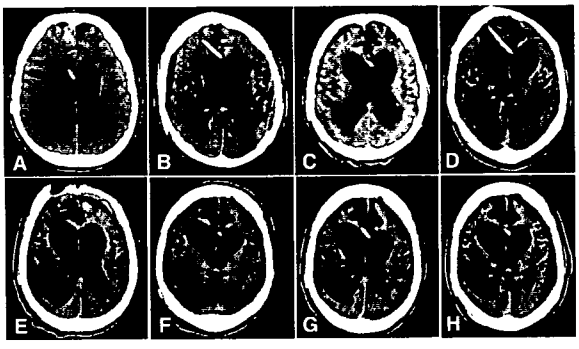

Figure 1. Non-enhanced serial CT scans of patient #1 after start of PPS administration. A. 3 months; **B.** 12 months; **C.** 15 months; **D.** 24 months; **E.** 30 months; **F.** 34 months; **G.** 40 months; **H.** 42 months. Note the progression of brain atrophy on initial scans with little changes after 24 months post-PPS. Subdural fluid collections over one or both hemispheres are seen on most scans.
CT: Computed tomography; PPS: Pentosan polysulfate.

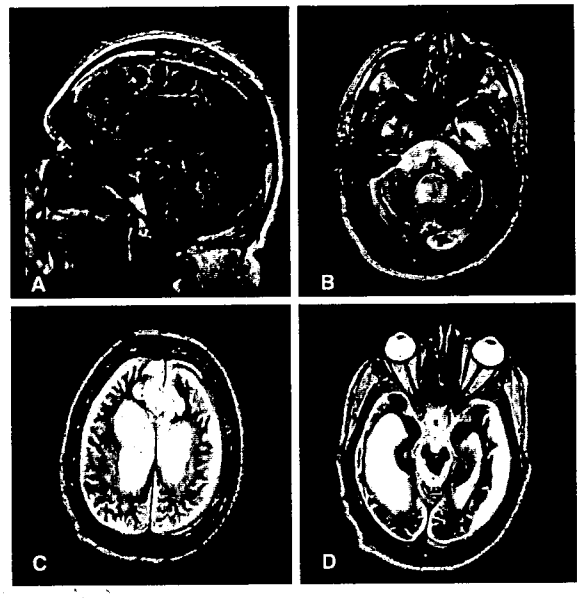

Figure 2. MRI scans of patient #1 42 months after start of PPS administration. Note advanced atrophy of brain stem, infra- and supratentorial structures, as well as a left-sided subdural fluid collection (without clinical correlation).
MRI: Magnetic resonance imaging; PPS: Pentosan polysulfate.

deficits are observed clinically and brain scans remain normal or show very little atrophy. At a later stage of the disease, the neurological deficits reach their full extent and remain stable, while brain atrophy still progresses. Eventually, if a patient is surviving long enough, brain atrophy will reach stable levels and stop progressing. This sequence of events seems typical for most of the long-term survivors on PPS, as illustrated in the above case.

Another male patient at the age of 18 years presented with a 12-month history of mood disturbance and subsequent ataxia, dysarthria, myoclonus and memory disturbance [86]. MRI scanning showed high signal in the pulvinar. The clinical diagnosis of vCJD was confirmed by a positive tonsil biopsy. Eight months after diagnosis, the patient did not speak voluntarily, was disorientated, but obeyed one-stage commands, was incontinent and dependent for all activities of daily living. A percutaneous gastrostomy tube was used for feeding, although the patient could still swallow a soft diet. The patient was no longer able to walk or transfer independently from bed to chair. Spontaneous myoclonic jerks were observed in all four limbs. This patient underwent stereotactic implantation of a right ventricular catheter and subcutaneous infusion pump (Synchromed EL, Medtronic). Repeated surgery a few days later was necessary to correct the position of the catheter. Intraventricular PPS infusion was started at an infusion rate of 1 µg/kg/day and the dose was escalated over the course of 2 weeks to 11 µg/kg/day without complications. PPS was increased 1 year later to 32 µg/kg/day without adverse effects. Reassessment 31 months after start of PPS treatment demonstrated minor clinical deterioration. The patient remained confined to either a chair or bed and was fully dependent for all activities of daily living. He was still able to take small amounts of soft diet orally, but was fed mainly via the gastrostomy tube. This vCJD patient has survived for 51 months after the onset of his clinical illness and for 31 months after start of PPS infusion. The dose of 32 µg/kg/day appears safe and well tolerated with no adverse effects such as seizures or subdural collections. In the first 18 months after PPS administration, the patient showed some progression of neurological symptoms, with subsequent stabilisation in his clinical conditions thereafter [86].

Whittle *et al.* (2006) [87] described the case of a 39-year-old female who presented with a 9-month history of psychiatric disturbance. MRI scan demonstrated high signal in the pulvinar, and tonsilar biopsy showed accumulation of PrP^{sc} in the germinal centers, both consistent with a diagnosis of probable vCJD. At the time of insertion of bilateral frontal ventricular catheters and implantation of the programmable drug infusion pump (Synchromed EL, Medtronic), the patient was alert but confused, ataxic but able to walk, and had neither incontinence nor involuntary movements. PPS infusion was commenced 1 week after surgery, 1 year after the onset of the initial clinical symptoms. The dosage was increased over 18 days from 1 to 110 µg/kg/day.

There were no immediate adverse effects from treatment. Serial CSF sampling via the reservoir revealed no intraventricular bleeding and MRI scan 2 months post-surgery was unchanged, with no evidence of haemorrhage. However, there was an inexorable clinical

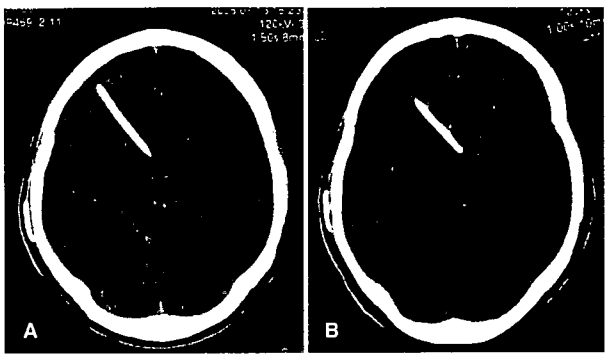

Figure 3. Non-enhanced CT scans of patient #17 1 month (A) and 7 months (B) after start of PPS administration. Note the clinically silent subdural fluid collections (mostly over the right hemisphere) seen 7 months after start of PPS.
CT: Computed tomography; PPS: Pentosan polysulfate.

decline with progressively worsening gait and truncal ataxia, and deterioration in speech and progressive cognitive decline were documented by serial neuropsychological assessments. Approximately 2 months after PPS was started, the patient had a series of tonic–clonic seizures, which were treated with intravenous benzodiazepines and sodium valproate, with prompt control of seizures. The PPS infusion was stopped. A range of investigations, including CT scan and CSF analysis, were normal. Over several days her condition stabilised. After 1 week the PPS infusion was resumed at 10 μg/kg/day and 6 days later increased to 25 μg/kg/day. A higher dosage was not given because of the possibility that the PPS had caused the seizures, although these may have been related to the disease itself. Subsequently, the condition deteriorated progressively to a state of akinetic mutism and the decision was made to stop PPS after 4 months of infusion. The patient died 3 weeks later due to infection, with a total duration of illness of 16 months. Post mortem was not carried out [87].

A Medical Research Council monitoring and observation study on seven patients receiving PPS has been recently carried out [102]. It concluded that intraventricular PPS does not cause any severe side effects, but that there are also no clear benefits of PPS treatment in halting disease progression. The study recommended further experimental work in animals to investigate PPS effects on survival and to show the extent to which PPS penetrates and spreads throughout the brain. In addition, a formal prospective longitudinal standardised follow-up study was recommended. It was underscored that intraventricular PPS itself does not carry a high probability of side effects after long-term usage, although there may be some surgery-related complications. Loss of brain function continues after PPS treatment has started and, where measured by imaging, loss of brain tissue also continues. The study also shows that intraventricular delivery might provide a long-term alternative route for other future therapies that cannot enter the CNS by oral or intravenous routes [102].

Since January 2003, a total of 26 patients with different TSEs have undergone surgery and continuous intraventricular administration of PPS. Anonymised clinical and follow-up data are presented in Table 1. The most important clinical finding is the safety of PPS administration to the cerebral ventricles. The maximum tolerated dose of PPS has not been reached. There were no cases with side effects clearly attributable to PPS, even in patients receiving 220 μg/kg/day.

Focal seizures have been observed in one patient receiving 11 μg/kg/day, and generalised tonic–clonic seizures have been observed in one patient with 110 μg/kg/day. It remains to be clarified whether these seizures were a side effect of PPS or of surgery, as in both cases they occurred months after start of PPS and during infusion with a stable dose of PPS.

Subdural collections are observed relatively frequently during administration of PPS (Figure 3); however, these usually resolve after discontinuing PPS for a short period of time, after which infusion can be resumed again. Except for the first case of PPS administration, where surgical drainage of the subdural collections was carried out due to lack of experience with their conservative management, no other PPS patients needed surgery for these collections.

It is unclear if a higher dose of PPS has a stronger effect and whether dose escalation should be continued at > 110 μg/kg/day. In most cases it seems that PPS administration results in a temporary halt or slowing of disease progression, but this conclusion is not based on objective measurements. PPS administration seems to be unable to reverse the clinical course of advanced disease and to achieve functional recovery of established neurological deficits.

Furthermore, surgery in the brain affected by TSE may result in a higher rate of surgical complications than usually encountered in comparable non-TSE cases. Brain atrophy may progress while PPS is administered, and it usually lags behind the progression of neurological signs and symptoms; however, there is no apparent correlation between the degree of atrophy and the clinical status of the patients. Results from the preclinical animal studies [67] suggest that cerebroventricular infusion of PPS should be commenced as early as possible after disease diagnosis and, if possible, before the occurrence of fixed neurological deficits.

5. Expert opinion and conclusions

Long-term administration of intraventricular PPS to the brain of TSE patients appears reasonably safe, based on experience with 26 cases. Preliminary clinical experience demonstrates extended survival in patients with vCJD receiving long-term PPS. Most vCJD patients are adolescents or young adults; therefore, vCJD will always be connected with younger age